Predation, community asynchrony, and metacommunity stability in cyanobacterial mats

Ethan C. Cissell[1*] & Sophie J. McCoy[1]

[1]Department of Biology, University of North Carolina at Chapel Hill, Chapel Hill, NC, USA

***Address correspondence to:**

Ethan C. Cissell

ecissell@unc.edu

(919) 843-7107

KEYWORDS:

Bacteriophage ; Bottom-Up ; Cellular Automata ; Coral Reef ; Cyanobacteria ; Fish ; Microbial Mat ; Natural History ; Molecular Ecology ; Species Interactions ; Top-Down ; Trophic Control

ABSTRACT

Holistically characterizing mechanisms that connect biotic context with patterns in persistence across levels of ecological organization requires integrating patterns of variability across scale. This is especially true in microbial communities, where relevant trophic interactions operate across disparate spatiotemporal scales. Here, we integrated observational, experimental, and theoretical approaches to unify local and regional ecological processes driving the dynamics of benthic cyanobacterial mats on coral reefs off the island of Bonaire, Caribbean Netherlands. Community and metacommunity dynamics of mats were tracked for 49 days alongside quantification of macropredation pressure from fishes. Viral interactions were interrogated using shotgun metagenomics and metatranscriptomics within a dying mat community to explore patterns in viral infectivity and prey population dynamics. Further, we employed a field experiment to test the hypothesis that enhanced predation would result in decreased mat persistence. Finally, we constructed a cellular automaton model to predict patterns in mat metacommunity dynamics across different scenarios of top-down and bottom-up control and dispersal. Cyanobacterial mat metacommunities were temporally stable across the study, stabilized by asynchrony in the dynamics of communities (~54% death rate in communities across 10 death dates). A total of 11 different reef fishes were documented foraging on mats, exhibiting heterogeneity in predation pressure among communities (72.8 mean bites per mat ± 111.2 bites SD) that likely contributes to the stabilizing asynchrony of community dynamics. Predation from reef fishes, though, may interact with other factors to influence mat community dynamics, as experimentally enhanced predation decreased the instantaneous mortality rate of mat communities over natural mat communities (-0.012 vs. -0.023). Viral linkage strength increased in decaying mat area over healthy mat area (median log abundance 2.41 vs. 2.27)

alongside decreases in prey population abundances. Theoretical simulations suggested that dispersal conveys a rescuing effect on mat metacommunity abundance under scenarios of strong trophic control, and dispersal is likely an important but unexplored driver of observed benthic cyanobacterial mat dynamics. We contextualize our experimental work with a collection of curated natural history observations and a unifying definition of benthic cyanobacterial mats. These data establish critical baselines and generate hypotheses relevant to the processes maintaining cyanobacterial dominance of reefs.

INTRODUCTION

Relevant mechanisms that drive changes in the abundance of organisms operate across many distinct spatiotemporal scales, and with variable frequencies and magnitudes (Connell et al. 1997), requiring integrative study to deal with this issue of variability across scale (Levin 1992). Theoretical developments in metacommunity ecology provide a robust framework for distilling the high dimensionality of complex species interaction networks - including all indirect and direct network linkages among populations - across local and regional scales into meaningful axes describing spatial stability vs. dynamism (Leibold et al. 2004). Global change and local stressors can modify interaction networks among competitors (McCoy and Pfister 2014) and trophically linked populations (Petchey et al. 1999, Falkenberg et al. 2013). Often, this elicits trophic guild-specific revisions to the predominance of competing trophic and competitive control mechanisms, especially in microbial systems, which makes it difficult to generalize traditional paradigms of top-down control and competitive network structure in multitrophic microbial assemblages in the current Anthropocene (Cissell and McCoy 2022b). The effects of shifting species linkages are further complicated by hierarchical interactive effects of

interspecific competition and predation in structuring prey populations (Paine 1966), as well as differential responses to changing environmental context among trophically linked populations (McCoy and Kamenos 2018). Collectively, this necessitates an explicit understanding of individual responses (McCoy et al. 2018), and all pairwise and interactive linkages (including indirect links such as interaction modifications [e.x., Wootton 1993]), to fully characterize mechanisms that connect abiotic and biotic context with patterns in population and community persistence (Hunter and Price 1992, Power 1992). Understanding how trophic links affect population dynamics and community structure via both direct and indirect effects is especially critical for effective intervention and control of nuisance organisms, such as blooms of toxic microorganisms (often dominated by algal taxa), which are dramatically increasing in abundance across aquatic ecosystems in response to Anthropogenically-mediated environmental change (Huisman et al. 2018). While planktonic cyanobacterial and eukaryotic algal blooms receive significant research and public attention, benthic blooms are underappreciated despite inhabiting and impacting some of the most threatened ecosystems globally.

Benthic cyanobacterial mats are dramatically increasing in abundance on coral reefs across the globe owing to the influence of both local and global stressors (reviewed in Ford et al. 2018). Coral reef cyanobacterial mats are complex microbial consortia, composed primarily of diverse bacteria, archaea, microbial eukaryotes, and viruses (Cissell and McCoy 2021, Biessy et al. 2021). Similar to typical microbial mat systems (Bolhuis et al. 2014), cyanobacterial mats are strongly cooperative communities, reliant upon metabolic handoffs and physiological synchronicity for persistence (Cissell & McCoy in review). The proliferation of cyanobacterial mats on coral reefs is thought to be both a cause and a consequence of the trajectory of reef degradation (Cissell and McCoy 2022b), with interactions among cyanobacterial mat cover and

major drivers of reef decline such as coral disease incidence (Cissell et al. 2022). Understanding the dynamics of cyanobacterial mats on coral reefs, then, represents a major challenge for coral reef ecologists and managers alike.

The focus of most work on coral reef benthic cyanobacterial mats has been on mat formation and growth, emphasizing the importance of bottom-up processes (i.e. release from bottom-up control via nutrient enrichment and warming) in driving the creation of cyanobacterial mats (Kuffner and Paul 2001, Albert et al. 2005, Brocke et al. 2015a). Little focus, however, has been given to the dynamics of mature (post-formation) cyanobacterial mat communities on coral reefs, and so the relative influence of top-down trophic interactions on mat community dynamics following mat establishment is largely unknown (Cissell and McCoy 2022b). Macrofaunal predation is generally considered to be a strong biotic filter preventing the establishment of microbial mats (Fenchel 1998). Microbial mats, then, generally only form in extreme environments that limit pressure from top-down forcing via physical exclusion of predatory macrobiota (Bolhuis et al. 2014). This logically suggests that top-down trophic interactions may strongly influence coral reef cyanobacterial mat bloom dynamics. Predatory interactions with both reef fishes and viruses have been previously documented with coral reef benthic cyanobacterial mats (Hewson et al. 2001, Cissell et al. 2019, Cissell and McCoy 2021), and correlative assessments of fish density and site-scale mat cover suggest some influence of predation on mat dynamics (Reverter et al. 2020). The spatiotemporal scales at which processes in this experimental system proceed allow dynamics across multiple scales of ecological organization, from populations to metacommunities, to be readily observable and amenable to experimental manipulation. Mat community patches on the reefs surrounding the Caribbean island of Bonaire form spatially distinct mats with discrete patch boundaries, which may be

longitudinally tracked macroscopically for evidence of predation and for broad community dynamics while efficiently solving the classic issue of community delineation and circumscription (Crowley 1978). Additionally, these distinct mat communities can be probed using molecular tools to probe relevant population scale functional dynamics and demography (Cissell & McCoy in review), and interactions with viral predators (Cissell and McCoy 2022a). Furthermore, recent molecular evidence from the comparison of average total nucleotide identity of Metagenome Assembled Genomes (MAGs) reconstructed among multiple spatially distinct benthic cyanobacterial mats on the fringing reefs of Bonaire revealed strong genomic conservation among mat communities, and suggests that cyanobacterial mats form true, dispersal-linked metacommunities on reefs (Cissell & McCoy in review).

Here, we integrate observational, molecular, and field experimental characterizations of local trophic interactions with documentation of spatial dynamics at multiple spatial scales and theoretical modeling simulations to understand and unify local and regional ecological processes driving the dynamics of benthic cyanobacterial mats on coral reefs off the island of Bonaire, Caribbean Netherlands. Natural community and metacommunity dynamics of cyanobacterial mats were tracked photographically alongside observational and next-generation molecular documentation of macro- and micropredation from fishes and viruses, respectively. Further, we employed a field coring experiment (simulated wounding) to test the hypothesis that enhanced predation would result in decreased mat persistence via a strong community response to top-down pressure (Fenchel 1998). Finally, we constructed a cellular automaton model to predict patterns in mat metacommunity dynamics across different scenarios of top-down and bottom-up control and dispersal. By pairing a longitudinal characterization of the structural state of mat landscapes and interaction network linkages with experimental manipulations of predation and

theoretical simulation, we can begin to contextualize and link patterns observed in space and time to the trophic processes generating structural dynamics across scales of ecological organization in cyanobacterial mats.

MATERIALS & METHODS

Tracks of natural and experimentally cored cyanobacterial mat communities, and assessment of metacommunity dynamics

Benthic cyanobacterial mats were tracked along a stretch of reef (146.2m straight-line length) on the southern leeward side of Bonaire, Caribbean Netherlands, in the Caribbean Sea (surveilled reef stretch extended from N12° 06.083' W68 17.269' to N12° 06.201 W68 17.328'). On 28 unevenly distributed unique sampling days spanning a total duration of 47 days (23 May 2019 – 09 July 2019), we took repeat, scaled photographs of 26 mats of the dominant orange-red morphotype (Appendix S1: Figure S1) using an integrated-camera PVC monopod (1m height). To establish which mats would be targeted for repeat sampling, mats growing on sediment in a ± 4m depth band (10 - 18m depth) were marked along a transect at 14m depth parallel to the reef slope. Although mats are also ubiquitous on hard substrate and living benthos (Ritson-Williams et al. 2005, Cissell et al. 2022; Appendix S1: Figure S2), only mats growing on sediment were marked to gain a better baseline understanding of mat bloom dynamics in the absence of any influence of competition/facilitation from close association with macro-benthic organisms. Individual mat communities were defined as spatially distinct mat individuals with discrete patch boundaries from other entire mats (Appendix S1: Figure S1). Generally, several meters of reef separated individual mat communities. Mats were semi-permanently marked with two plastic

stakes and a PVC place-marker to allow for repeat monopod placement over the 49 days and to facilitate intra-image georeferencing in later analyses.

To explore the effects of disturbance from top-down forcing on mat dynamics, an additional 27 mats were identified as described above and a 1.3cm diameter core was experimentally removed from both the interior of the mat and from the mat's border using a PVC corer and forceps to simulate predation from reef fishes (core size predetermined from mean size of bite scarring measured in mat images taken in Jan 2019; Cissell, Pers. Obsv.). These mats were marked and repeatedly photographed as described above.

Dynamics in the site-scale cover of sediment-bound cyanobacterial mats was used as a proxy for assessing mat metacommunity dynamics at our study site. Mat cover across a depth range of 7m – 19.8m across the length of the study site from 5 separate sampling dates was assessed in 204 haphazardly placed photoquadrats ($0.25m^2$) from manual annotation of 50 randomly placed points per quadrat in *CoralNet* beta. Only cyanobacterial mats growing on sediment were annotated as cyanobacterial mat in this analysis – mats overgrowing hard substrate were annotated as EAM. Because these functional groupings were intentionally designed differently from conventional grouping structures to capture and track cyanobacterial mat dynamics specifically on sediment, we make no inference on the cover of other benthic groupings and dissuade use of these benthic cover data toward alternative purposes to those stated herein.

Surveys of macropredatory pressure

Grazing rates from reef fishes were quantified using diver-independent fixed-point timed behavioral observations using either a Nikon Coolpix W300 or a GoPro Hero4 equipped with a

red filter. Observations were made on 22 individual mat communities across 5 sites found between 13.2m and 17.3m depth (mean 14.9m) between the hours of 10:00 and 16:00 corresponding to the peak feeding time of most grazing fish species in the Caribbean (Bruggemann et al. 1994b) for a mean observational duration of 26 minutes per mat. Survey cameras were placed on reef substrate away from the focal mat such that the entire mat area was visible and surveilled within the frame. The first minute of each behavioral observation period was removed from analysis to allow the behavior of the fish community to acclimate to camera presence. During video analysis, each bite that visibly removed biomass was counted, and the identity of the species biting the mat was recorded. Foraging by spotted goatfish (*Pseudupeneus maculatus*) and yellow goatfish (*Mulloidichthys martinicus*) individuals mostly consisted of the following feeding modes: shovel, push, and skim surface (Krajewski et al. 2006). Though these goatfish individuals were likely not foraging directly on cyanobacterial mat biomass, their foraging activity disturbs mat biomass similarly to predation from other reef fishes actively grazing cyanobacterial mat biomass, and so data on their foraging are presented as 'bites', where each individual foray was counted as a single 'bite' regardless of duration or magnitude.

Sampling of a senescent mat and overview of shotgun metagenomic and metatranscriptomic sequencing

Samples were collected from a single macroscopically decaying cyanobacterial mat individual found on sediment at 12.6m depth for molecular inference of viral infection dynamics (micropredation) associated with visible mat decay (Appendix S1: Figure S3). Meta'omic sequencing-based approaches provide robust indirect quantification of trophic interaction direction and strength for viruses of cellular microorganisms (Coutinho et al. 2017, Cissell and

McCoy 2022a). Samples were collected on 04 June 2019 at 09:58 Atlantic Standard Time from 3 points across an imaginary transect spanning the senescing mat individual, including samples from the following mat areas: the visibly healthy portion of the mat (hereafter '*Living*'), the mat area at the immediate edge between healthy and senescent mat biomass (hereafter '*Border*'), and the visibly senescent portion of the mat (hereafter '*Decay*'). Four replicate samples per broad mat area were collected, for a total of 12 collected samples. The sampled mat was photographically followed as described above post-sampling for a total of 17 time points spanning 33 days (followed until 09 July 2019). The remainder of the visibly healthy mat portion had begun to decay after 10 days post-sampling, and most of the mat area had collapsed after 18 days post-sampling (Appendix S1: Figure S4).

Samples collected from within a mat area (4 samples per mat area) were pooled to account for potential intra-mat spatial variation within a grouped area (Cissell and McCoy 2021) for a total of 3 samples prepped for meta'omic sequencing. Bulk DNA and RNA extraction and the preparation of libraries for sequencing were performed following protocols previously described (Cissell and McCoy 2021; Cissell & McCoy in review). Briefly, the E.Z.N.A Soil DNA Kit (Omega) was used to extract bulk DNA from pooled samples, while a TRIzol LS (ThermoFischer) extraction protocol was used to extract bulk RNA from pooled samples. The NEBNext Ultra II DNA and RNA Library Prep Kits for Illumina (New England Biolabs) were used to prepare libraries from DNA and cDNA templates respectively. Prior to RNA library preparation, ribosomal RNA (rRNA) was depleted using the NEBNext rRNA Depletion Kit (Bacteria; New England Biolabs). Metagenome reads will hereafter be referred to as 'DNA reads' and metatranscriptome reads (cDNA) will hereafter be referred to as 'RNA reads' for ease of interpretation. Libraries were duel-indexed, and sequenced on an S4 flow cell on an Illumina

NovaSeq 6000 using a 300 cycle kit (paired-end 150bp chemistry). This sequencing generated a total of ~2.6 billion reads across all samples (Appendix S1: Table S1).

Paired-end DNA reads were demultiplexed and quality trimmed to a minimum Phred quality score threshold of 20, and a minimum length threshold of 100bp using *TrimGalore* ver. 0.6.6 (with *Cutadapt* ver. 1.18). Reads were mapped to a soft-masked version of the human genome (HG38; patch release 13 (2019/02/28), GenBank Accession#: GCA_000001405.28) using *Bowtie2* ver. 2.3.4.1 (Langmead and Salzberg 2012) to remove any possible human contamination (>99.99% of reads retained; Appendix S1: Table S1). *FastQC* ver. 0.11.9 was used to assess quality of reads following quality control. A *k*-mer redundancy estimator was implemented on *31*-mers pulled from a query size of 10,000 quality-controlled reads using a 1,024 sub-sampling strategy with *Nonpareil 3* ver. 3.304 (Rodriguez-R et al. 2018) to assess sequencing coverage (Appendix S1: Figure S5, Table S2). cDNA reads (metatranscriptomes) had adapters removed and were quality trimmed to a Phred quality score of 20 and a minimum length threshold of 50bp using *TrimGalore*. rRNA reads that were not removed during library preparation were removed in-silico using *SortMeRNA* ver. 4.2.0 (Kopylova et al. 2012). The quality of quality-controlled RNA reads was assessed using *FastQC*. These sequencing data are accessible under BioProject accession number PRJNA632569 in the NCBI sra database.

Metagenomes were assembled *de-novo* for each sample's quality controlled read pairs independently using the *IDBA-UD* assembler (Peng et al. 2012). The quality of resulting contigs and scaffolds was assessed using *QUAST* (Gurevich et al. 2013; Appendix S1: Table S3). Following assembly, scaffolds exceeding 1.5kpb in length were first binned unsupervised from each individual assembly using *Metabat2* ver. 2.15 (Kang et al. 2019), *Vamb* ver. 3.0.2. (Nissen et al. 2021), and *Maxbin2* ver. 2.2.7 (Wu et al. 2016) using default parameters for each algorithm

and using mapping data from each read set per assembly. Bins generated using these three unsupervised methods were coalesced into a single bin set using *DasTool* ver. 1.1.2 (Sieber et al. 2018) with a score threshold of 0.5. Bin outputs from *DasTool* were subsequently subject to stringent manual (supervised) refinement within *Anvi'o* ver. 7 (Eren et al. 2015) by evaluating patterns of variability in tetranucleotide frequency, GC bias, and differential coverage predictors. Redundancy and completeness of genomes (from presence and counts of single-copy core genes) were assessed within *Anvi'o*. Bins were then dereplicated across assemblies at 95% identity using *dRep* ver. 3.2.0 (Olm et al. 2017), generating a nonredundant$_{95\%}$ database of shared bins across all assemblies. Broad taxonomic placement of bins was inferred using *GTDB-Tk* ver. 1.5.0 using default parameters against GTDB release 06-RS202 (2021-04-27 update), and the 2 predicted cyanobacterial genomes were retained for further downstream analyses, and assigned as putative cyanobacterial MAGs (completion >50% and redundancy < 10% for each). Useable 16S rRNA gene regions could not be detected from either cyanobacterial MAG, however *FastANI* ver. 1.32 (Jain et al. 2018) with a fragment length of 1,000 was used to compare recovered cyanobacterial MAGs to each other, and to previously curated cyanobacterial MAGs from cyanobacterial mats from Bonaire (Cissell & McCoy in review). Additionally, a pangenomic based approach was used to infer the lineage of the cyanobacterial MAG with a global ANI less than 99% to previous recovered cyanobacterial MAGs from reef benthic cyanobacterial mats (DAL_MAG_7) using *SANS serif* ver. 2.1_098A with a *k*-mer length of 31 and a strict maximum weight subset (approximates classic tree). Lineage was inferred against 84 *complete* cyanobacterial genomes pulled from NCBI.

Viral sequence curation, integrative host determination, and abundance mapping

Initially, putative viral sequences were defined in scaffolds from each individual assembly (dsDNA and ssDNA viruses) using reference-based definitions (recognition of viral hallmark gene homologs and the enrichment of viral signature proteins) using *VirSorter2* ver. 2.2.3 (Guo et al. 2021), with predicted scaffolds exceeding 2.5kbp in length and exceeding a score threshold cutoff of 0.5 retained. *CheckV* ver. 0.8.1 (Nayfach et al. 2021) was used to define host boundaries in putative prophage sequences and assess quality and completeness of retained viral scaffolds. *DRAMv* ver. 1.2.2 (Shaffer et al. 2020) was subsequently used to annotate predicted Open Reading Frames (from *Prodigal* [Hyatt et al. 2010]) using homology searches against PFAM, dbCAN, RefSeq viral, VOGDB, and MEROPS. Viral scaffolds were then stringently manually screened using viral and host gene counts from *CheckV*, gene-level annotations from *DRAMv*, hallmark gene counts from *VirSorter2*, and scaffold scores following previously benchmarked protocols (Guo et al. n.d.). The manually curated viral scaffolds were clustered at 95% sequence identity within and across assemblies using *CD-HIT-EST* ver. 4.7 (Li and Godzik 2006), which created a shared nonredundant$_{95\%}$ database of 811 vOTUs across all samples (vDEATH database). The nonredundant vOTUs in vDEATH were further validated using non-reference-based Hidden Markov Model (HMM) searches using *VIBRANT* ver. 1.2.0 (Kieft et al. 2020) with the *–virome* flag. A total of 608 of the 811 vOTUs were validated using *VIBRANT* (75.0% of identified vOTUs$_{95\%}$).

Putative cyanophages were predicted via integrative prognostic computational prediction of host-viral linkages. A total of 3 approaches were integrated, including the following methods: CRISPR-spacer:protospacer matching, oligonucleotide frequency screening, and host-viral homology matching. *MinCED* ver. 0.4.2 (Bland et al. 2007) was used to predict CRISPR spacer regions on the 2 cyanobacterial MAGs recovered in this study. These identified CRISPR regions

were subsequently packaged into a custom nucleotide database, and viral scaffold protospacers were queried against this CRISPR database using *BLASTn* with previously benchmarked optimum search standards across the spacer length (*BLASTn* – short; maximum E-value 1; gap opening penalty 10; gap extension penalty 2; mismatch penalty 1; word size 7; (Edwards et al. 2016)). Only those matches with ≤ 1 mismatch were retained. The frequencies of shared *k*-mer (using *25*-mers) among viral scaffolds and cyanobacterial MAGs were obtained using *PHIST* ver. 1.0.0 (Zielezinski et al. 2022), discarding pairings that exceeded an adjusted p-value of >0.001 and possessing lower frequencies of shared *25*-mers than the global median (305.5 unique shared *k*-mers). Finally, *BLASTn* was used to query raw viral scaffolds against a custom nucleotide database of cyanobacterial MAGs from this study, retaining hits above a >70% minimum nucleotide identity, ≥75% coverage over the viral scaffold length, ≥50 bit score, and e-value ≤ 0.001 (Li et al. 2021). The single best hit from each computational prognostic method was screened and retained. Predictions across methods for each unique viral scaffold were integrated and compared using custom scripts that retained hits with consensus across methods and resolved multiple host predictions using the following ranked criteria: 1) best CRISPR spacer-protospacer match; 2) nucleotide sequence homology match; and 3) similarity in oligonucleotide frequency. A total of 352 vOTUs were predicted to infect the dominant cyanobacterial MAGs recovered in this study.

The relative abundance of both cyanobacterial MAGs and vOTUs was assessed from read recruitment profiles obtained from global *Bowtie2* alignments using *CoverM* ver. 0.6.1. Copies Per Million (CPM) values (Wagner et al. 2012) were subsequently calculated using raw read counts and lengths using custom scripts. Virus-Microbe Ratios (VMRs) were calculated as the ratio of CPM normalized abundances of putative cyanophage to linked hosts, where total phage

and host abundances sum to 1e+6. RNA reads were similarly mapped to vOTUs and cyanobacterial MAGs using *BWA-MEM* ver. 0.7.17 (Li 2013), generating bulk activity profiles (multi-mapping reads excluded). Raw count profiles from each sample were normalized to Transcripts Per Million (TPM) values using custom scripts by querying high-quality alignments to gene-level feature data, creating feature tables containing the relative abundance (TPM) of each vOTU and cyanobacterial MAG in the metatranscriptome. TPM normalization utilized the summed length of predicted ORFs on each feature (from *Prodigal*), rather than total genomic length for sequence length standardization. Virus-Microbe Activity Ratios (VMARs) were calculated like VMR as described above (Cissell and McCoy 2022a). Abundance-normalized TPM estimates were created by dividing TPM normalized expression data by CPM normalized abundance data obtained from metagenomes (normalization procedure described above).

Cellular automaton model overview, parameterization, and simulation procedure

Model simulations using C^{++} were used to predict patterns in mat metacommunity dynamics across gradients of top-down and bottom-up control and dispersal, motivated by the need for a mechanistic understanding of the decoupling between nutrient control and management outcomes for standing mat cover on reefs (Model code provided in Github link for reviewers). The model presented is based on the cellular automaton model previously presented in McCoy et al. (2016). The simulated site was represented by a grid of 5,000 x 5,000 cells, with each grid cell corresponding to an area of reef $50mm^2$ in size (roughly corresponding to average bite sizes measure in Jan. 2019; Cissell, Pers. Obsv.) for a total modeled area of $1{,}250m^2$. Opposing edges in the model grid were connected to wrap the grid into a torus to avoid edge effects (McCoy et al. 2016). The bare grid represents colonizable reef substrate. Coral reef

cyanobacterial mats have been observed overgrowing most possible benthic substrates, both biotic and abiotic (Appendix S1: Figure S2), and therefore no distinction is made among benthic substrates to match the assumption of equal occupational probability across substrate types. A single model time step is equivalent to a period of 24hrs, and each model was run for a total of 365 time steps for a total duration of a 1-year time period per simulation.

The starting simulation grid matrix was generated in QGIS ver. 3.16 (Hannover). A raster layer of bare substrate was randomly populated with cyanobacterial cells following a binomial distribution with an N of 1 and a probability of 0.2, creating a starting site-scale abundance of 20% cyanobacterial mat. This generated grid was input as the starting grid for every model run.

A total of 64 unique parameterizations were simulated, including all possible permutations of 4 levels per parameter across 3 unique parameters. Parameters that were varied in this model were mat DISPERSAL, mat GROWTH RATE, and DISTURBANCE (broadly encompassing macropredation, micropredation, and goatfish disturbance each with independent probabilities). Levels of each parameter were broadly classified into the following bins: Zero, Low, Medium, and High. Parameterizations correspond to a probability of each event occurring within a model time step. Exact numerical parameterizations for each parameter are provided in Appendix S1: Table S4. For each model ‘decision’, a random number from 0-1 was pulled from a random number generator and compared to the parameterized probability of each event to determine the outcome of the event. Within a time step, focal cells were chosen at random. Focal cells that were not occupied by cyanobacterial mat could have mat successfully dispersed into them with probability DISPERSAL, filling the cell with mat when successful. It should be noted here that the process of dispersal is modeled as a generative colonization event, and not necessarily as population connectivity among spatially distinct mat communities. Focal cells that

were instead occupied with mat and that had an empty neighboring cell (pulled at random) could then grow into that empty neighboring cell based on GROWTH RATE. Each focal cell could only grow into a single empty neighboring cell per time step (maximally one growth event per focal cell per model step). Following this growth step, focal cells that were occupied were then subject to a possibility of disturbance from goatfish, macropredation (from consumptive reef fishes), and micropredation based on each respective probability from DISTURBANCE. Either when a focal cell had been disturbed (became empty substrate) or passed all disturbance events without success (remained mat), a new focal cell was chosen (without replacement) and the loop continued. Only one disturbance event per focal cell per time point was possible. Total counts of bare substrate and mat cells were tallied at the end of each time step. Model outputs (abundances from counts/total) are presented as means and standard deviations from 100 independent model runs per parameterization combination.

Statistical procedures

All statistical analyses were conducted using the R programming language (ver. 3.6.2) implemented in RStudio (ver. 1.2.5033). Data visualization was performed using *R::ggplot2*(ver. 3.3.3). Model assumptions for all models (across all chosen likelihoods; unless otherwise specified) was assessed from model residuals graphically using *R::DHARMa* (ver. 0.3.3.0).

To assess metacommunity dynamics at the study site across the study duration, site-scale cover of cyanobacterial mats was modeled against both benthic sampling date and depth of photoquadrat (n=204) as predictors using linear models (Gaussian likelihood). The distribution of photoquadrats across depths across sampling dates was initially assessed graphically (Appendix S1: Figure S6). A nested model structure was fit including an additive or interactive

effect of both predictors. The interactive terms were not significant (all pairwise $p > 0.05$; overall term $F = 1.29$, $df = 4$, $p = 0.27$), and a likelihood ratio test - conducted to determine if adding the complexity of the interaction term improved model fit - suggested that the interaction term could be dropped ($p = 0.27$). Parameter estimates and error structures presented are from the additive model. Post-hoc pairwise Wilcoxon Rank Sum Tests with Bonferroni p-value corrections were used to assess pairwise differences among levels of sampling date.

To test for an effect of the experimental coring treatment on the overall probability of a mat (n=53) dying during the study period, a binomial Generalized Linear Model (GLM) was fit, where the response variable was a 0 or 1 corresponding to if a mat died during the study period ("0") or not ("1"). Both 'Treatment' and 'Start Date' and their interaction were included as predictors in the model. A Kruskal-Wallis test was used to test for a significant difference in start dates among treatments. No significant difference in start date among treatments was detected (K-W$\chi^2 = 0.02$, $df = 1$, $p = 0.88$), however a likelihood ratio test between the fully interactive model and a model fit without 'Start Date' as a predictor suggested that "Start Date" should be included in the analyzed model ($p=0.02$). The significance of fixed effects in each model, including that of the interaction term, were assessed using Type II Wald's χ^2 tests conducted using car [3.10-10]::Anova. The interaction term between Treatment and Start Date in this interactive GLM was not significant ($df = 2$, $F = 1.63$, $p = 0.21$), offering further verification that there was no significant difference in start dates between treatments. The instantaneous mortality rates of mats in each treatment of the field simulated predation experiment were predicted by fitting exponential decay curves (logistic regression) to the experimental data. A quasibinomial GLM was fit to the binomial response variable of mat death (structure described above) against observation duration in days without intercepts. The model was fit using the quasibinomial

family distribution with a log link function, with separate parameters estimated per treatment. Significance of model terms was assessed using a Chi-Square test.

To model bite count on cyanobacterial mats, we fit a generalized linear mixed effects model using glmmTMB::glmmTMB (ver. 1.0.2.1) with a negative binomial distribution and a log link, treating site and fish species as fixed predictor variables and allowing the intercept to vary by mat identity nested within site, including an offset of the log of video duration (in seconds). Initial phase and terminal phase of species, where available / applicable, were fit as separate levels of the predictor "Species" and were not separately included as a "Phase" predictor variable because different phases were not observed / not applicable for all species observed consuming cyanobacterial mat biomass. A Type II Wald's χ^2 test was used to assess significance of fixed effects parameter estimates. Bites from taken by bicolor damselfish were removed from this model because the direct effects from their bites are small in magnitude (minimal biomass removal).

RESULTS

Cyanobacterial mat metacommunities are temporally stable, with asynchronous instability of component communities.

The dynamics of spatially distinct individual benthic cyanobacterial mat communities and the broader site-scale metacommunity were photographically monitored for 49 days along a stretch of reef 146.2m long in straight-line length on the leeward fringing reefs of Bonaire. The metacommunity at this site was temporally stable across the study, slightly increasing after initial sampling to a consistent cover (Fig. 5.1a; LM; df = 4; F = 4.79; p = 0.001; PWRST p=0.02, 0.0002, 0.042 between initial and 2nd, 3rd, and 4th sampling, all other p > 0.05). Mean

metacommunity cover across the study duration was 19.6% ± 4.94% SD (Fig. 1a). Site-scale cyanobacterial mat cover showed a significant trend with depth, increasing by ~1.2% benthic cover per meter depth increase (LM; $y = 0.012x - 0.04$; $df = 1$; $F = 9.42$; $p = 0.002$; Appendix S1: Figure S7). High abundances of cyanobacterial mats have been reported at mesophotic depths in other reef ecosystems (Sellanes et al. 2021) and on the mesophotic reefs around Bonaire (van Heuzen 2015). Additionally, this study site is marked by the presence of a sand channel at deeper depths connecting a double reef structure whose flanking regions provide protected habitat for cyanobacterial mat proliferation, making this trend with depth not surprising.

Alongside documented metacommunity stability across the study period, component communities showed remarkable volatility (Fig. 1b). At the end of the 49-day study period, 53.8% of the tracked cyanobacterial mat communities (considering only unmanipulated mats; 14 / 26 mat individuals) had died across 10 unique death dates (Fig. 1b), indicating a high degree of asynchrony in the dynamics of individual component communities comprising this mat metacommunity.

Experimental wounding does not increase likelihood of mat death, and decreases predicted instantaneous mortality rate of mat communities.

To test for an effect of macroscale disturbance (most closely approximating direct effects from predation by consumptive reef fishes) on the dynamics of benthic cyanobacterial mats, 27 mats were experimentally cored in the field, representing a ‘wounding’ treatment over unmanipulated mats. Motivated by previous work demonstrating a strong antagonistic effect of predation pressure on the establishment and persistence of experimental microbial mats (Fenchel 1998), we hypothesized that enhanced predation would result in decreased reef cyanobacterial

mat persistence via a strong community response to top-down pressure. We found little support for this hypothesis, with no significant difference in the overall probability of mat community death over unmanipulated mats (GLM, F = 0.114, df = 1, p = 0.74; Fig. 2a). Interestingly, however, cyanobacterial mats in the coring treatment were predicted to survive longer, having a significantly lower instantaneous mortality rate (-0.012 [-0.024 - -0.005 97.5% CI]) than mats that were left unmanipulated (-0.023 [-0.041 - -0.011 97.5% CI]; GLM, dev = 8, df = 2, p < 2.2e-16), suggesting that moderately increased predation pressure increases mat longevity (Fig. 2b).

Macropredation pressure is heterogenous among mat communities, and varies by predator identity

Diver-independent fixed-point behavioral assays were deployed on 22 spatially distinct cyanobacterial mat communities across five different reef sites to identify relevant sources of macropredation and quantify rates of predation pressure. A total of 11 different fish species were documented to have foraging behavior that impacted cyanobacterial mat biomass, with both initial phase and terminal phase individuals from 3 species observed grazing on cyanobacterial mat biomass (Fig. 3). While bite pressure differed significantly by fish species identity (chisq = 39.2; df = 13; p = 0.0002), no significant difference among sampled sites was detected (chisq = 21.59; df = 4, p = 0.81; Appendix S1: Figure S8). Predation pressure among mats, however, was highly variable (72.8 mean bites per mat ± 111.2 bites SD; GLMM random effect variance 3.12 ± 1.77 SD), overall suggesting heterogenous macropredation pressure from reef fishes within (i.e. heterogenous among individual mat communities), but not necessarily among, mat metacommunities (i.e. relatively homogenous among sites). Mean bite rate (bites*min^{-1}) across all species taken on cyanobacterial mat communities was 0.23 ± 0.92SD. Though greatest in

frequency (Fig 3), bites taken by the Bicolor Damselfish (*Stegastes partitus*) were not of as great of magnitude (i.e. did not remove as much visible mat biomass) as bites by other fish species. Similarly, bites taken by larger predators such as the French Angelfish (*Pomacanthus paru*) and the Queen Parrotfish (*Scarus vetula*), though fewer in frequency, were of much greater magnitude and removed significant biomass with each bite. The number of bites taken by initial phase Striped Parrotfish (*Scarus iseri*; mean 13.8), Princess Parrotfish (*Scarus taeniopterus*; mean 6.2) and Redband Parrotfish (*Sparisoma aurofrenatum*; mean 2.0), were generally higher than those taken by terminal phase individuals (means 7.3, 2.8, and 0.3, respectively). However, again, an effect of species changes the magnitude of each bite, with greater biomass removal from terminal phase individuals.

Median viral abundance increases in decaying mat area, with an inverse pattern detected between the dominant cyanobacterial MAG and corresponding VMR.

A transect across a visibly decaying cyanobacterial mat (Appendix S1: Figure S4) was sampled to better understand patterns in micropredation associated with mat decay. Cyanobacterial MAGs were manually curated from individually assembled metagenomes, with a total of 2 cyanobacterial MAGs recovered. The dominant cyanobacterial MAG from the living sample (DAL_MAG_7; length 8.3Mbp; 83.1% Completion; 2.82% Redundancy) had a global ANI of 87.6% to the dominant cyanobacterial MAG assembled from a morphotypically similar cyanobacterial mat from Bonaire (Cissell & McCoy in review), and an ANI of 87.5% to the other cyanobacterial MAG assembled in this study (DAB_MAG_2; length 7.9Mbp; 91.5% Completion; 5.6% Redundancy). DAB_MAG_2 had a 99.8% global ANI similarity to the dominant cyanobacterial MAG assembled in a morphotypically similar cyanobacterial mat,

indicating that this MAG likely represents an *Oscillatoria* sp(p). (Cissell & McCoy in review). Taxonomic placement of DAL_MAG_7 was inferred using a pangenomic similarity approach, with evidence for this MAG likely representing a member of the order Chroococcales (Appendix S1: Figure S9).

As in Cissell & McCoy (2022a), HMM searches and *BLASTp* with non-reference based HMM searches were implemented to extract viral signatures from individually assembled metagenomic scaffolds. A total of 811 shared nonredundant$_{95\%}$ vOTUs were recovered and manually curated, with a mean sequence length of 6,647bp. The abundance of each individual vOTU and cyanobacterial MAG was assessed across the transect of samples from global read recruitment profiles, revealing a higher median viral abundance associated with the *Decay* mat sample than the *Living* mat sample (median $\log_{10}$CPM 2.41 vs. 2.27 in the *Decay* vs *Living* sample respectively; Fig. 4b). The median abundance in the *Decay* sample was close to, but just under the 3rd quartile abundance from the *Living* sample (2.44 $\log_{10}$CPM), and the 3rd quartile from the *Decay* sample greatly exceeded that of the *Living* sample (2.88 $\log_{10}$CPM). Median abundance in the *Border* sample was the lowest of the 3 sampled areas (1.64 $\log_{10}$CPM), but had the highest maximal abundance (5.01 vs. 4.79 and 4.58 $\log_{10}$CPM in the *Living* and *Decay* samples respectively; Fig. 4b). Patterns in evenness of the viral community across this transect were graphically explored by creating rank-abundance curves of log transformed CPM normalized viral abundances (log+1 transformation). These plots revealed a general shift in the pattern of evenness in the viral community moving from the *Living* toward the *Decay* sample, specifically with an erosion of the long tail of the evenness plateau characterizing the *Living* sample toward an overall increase in the abundance but overall shortening (covered ranks; steeper slope) of the central plateau (Appendix S1: Figure S10).

The presence and proper treatment of zeros in sequencing space is an ongoing debate in bioinformatics and molecular biology in general (Quinn et al. 2019, Silverman et al. 2020). The relatively lower depth of sampling in the *Border* sample and *Decay* sample compared to the *Living* sample likely inflates the relative contribution of Sampling Zeros over Biological Zeros in viral CPM abundance space, especially considering the inherent difficulty in viral recovery from metagenomic samples with lower sampling depth (Silverman et al. 2020). To explore the influence of zeros on overall interpretations, viral sequences were subject to additional analyses on a subset of data which removed those sequences with zero counts across any of the samples (Appendix S1: Figure S11). Removing zeros exacerbated the patterns seen when zeros were included (Appendix S1: Figure S11), with median viral abundance in the *Decay* sample exceeding the 3rd quartile abundance in the *Living* sample (2.54 vs. 2.44 $\log_{10}$CPM respectively), and sharply raising the median abundance of viral sequences in the *Border* sample (1.82 $\log_{10}$CPM).

To further explore lineage-resolved patterns in viral:host linkages associated with these broad patterns discussed above, patterns in the raw abundances and ratios of abundances between the dominant cyanobacterial MAGs and their putative infecting cyanophages were specifically documented. Multiple computational prognostic strategies were integrated to resolve putative host-virus linkages. Interestingly, the VMR of the dominant cyanobacterial MAG from the *Living* sample sharply increased across the span of the transect (1.52 vs. 2.00 vs. 2.16 $\log_{10}$VMR in the *Living*, *Border*, and *Decay* samples, respectively; Fig. 5a), coupled to an inverse decrease in MAG abundance (4.30 vs. 3.56 vs. 3.40 $\log_{10}$CPM in the *Living*, *Border*, and *Decay* samples, respectively; Fig. 5b). Decreasing abundance of the dominant cyanobacterial MAG with mat decay would be expected given that Cyanobacteria are the dominant mat framework builders in

providing mat community physical structure (Stal et al. 1985, Cissell and McCoy 2021), and given the macroscopic manifestation of mat decay (Appendix S1: Figure S3). Patterns in the less dominant cyanobacterial MAG (DAB_MAG_2) were less predictable and showed no clear trend across the transect other than a general increase over its abundance in the *Living* sample (Fig. 5b).

Viral activity is higher at the border between apparently healthy and decaying mat tissue than within decaying mat tissue, and displays comparable patterns in VMAR with those in VMR.

While the median abundance of vOTUs was higher in the *Decay* sample than in the *Border* sample, recruitment of reads from recovered metatranscriptomes revealed that median vOTU activity was higher in the *Border* sample than in the *Decay* sample (median $\log_{10}$TPM 1.79 vs 1.59 in the Border and Decay samples, respectively; Fig. 4c). This difference in pattern between viral activity and abundance makes intuitive sense, as patterns in abundance contain a greater degree of relic effects than patterns in activity (shorter half-life of RNA over DNA). Higher viral activity at the border between apparently healthy and decaying mat tissue suggests an active response to a dynamic front of mat decay within the viral assemblage of mat communities.

Interestingly, lineage-resolved patterns in activity closely aligned with those presented from patterns in abundance (Fig. 5c,d). The ratio of activity ($\log_{10}$VMAR) between viruses and the dominant cyanobacterial MAG in the *Living* sample increased from 2.82 to 2.96 between the *Border* and *Decay* samples (Fig. 5c). Activity profiles of the subdominant cyanobacterial MAG in the *Living* sample and its viruses remained relatively constant (Fig. 5c,d).

Moderate dispersal conveys rescue effect to mat metacommunities even with strong top-down control.

A metacommunity cellular automaton model was employed to explore how different scenarios of bottom-up forcing, top-down control, and dispersal drive mat metacommunity dynamics. Scenarios at naturally unlikely extremes (i.e. zero top-down forcing or immense bottom-up control [zero growth]) generally showed outcomes well aligned with *a priori* assumptions, either saturating the metacommunity at 100% benthic cover or ending with the metacommunity going extinct, persisting at 0% benthic cover (Fig. 6). Model outputs suggest that even moderate levels of top-down control from predation can significantly reduce the relative benthic cover of mat metacommunities, with high levels of top-down control almost always driving metacommunity extinction without dispersal (Fig. 6). Interestingly however, strong dispersal potential conveys a rescuing effect on metacommunity persistence even in scenarios with relatively strong top-down and bottom-up control (mean equilibrium proportional abundance ~1.6% under High Predation, Low Growth, High Dispersal, and ~1.2% under High Predation, Zero Growth, and High Dispersal; Fig. 6). Moderate dispersal can still promote persistence, but at extremely low cover under strong control scenarios (~0.16% cover under H_Z_M scenario). Further, under more realistic scenarios (i.e. Moderate top-down and bottom-up control), strong dispersal potential can maintain metacommunity cover at values close to the starting abundance, mirroring patterns empirically observed in the field during this study period (Fig. 1, 6). This suggests that strong dispersal is an important mechanism driving mat metacommunity dynamics on reefs.

DISCUSSION

Decoupling of local and regional scale patterns

In comparison to persistent mat metacommunity stability, component mat communities displayed remarkable instability in physical space (Fig. 1). However, the temporal pattern of senescence of individual communities was highly asynchronous, occurring across 10 unique death dates (Fig. 1b). This asynchrony can strongly decouple patterns in community and metacommunity dynamics and mitigates the correlative strength between local community extinction risk and regional metacommunity extinction risk. Asynchrony in substructure component dynamics (i.e. decorrelation of population and community extinction and recolonization across axes of space and time) has long been appreciated as an important systemic stabilizing force in both metapopulation and metacommunity ecology, promoting stability in metacommunity biomass and ecosystem function by decreasing intra-scale variability of abundances (Paine and Fenchel 1994, Holyoak and Lawler 1996, Wilcox et al. 2017). Predation pressure can be an important force toward preventing synchrony among communities and promoting compensatory oscillatory dynamics in metacommunities, even in systems with strongly synchronizing dispersal (Howeth and Leibold 2013). However, the extent of these effects depends strongly upon predator niche, distribution of predation pressure in time and space, and context of abiotic environmental variability, as predators can antithetically promote species and spatial patch synchrony via spatial coupling of dynamics (Howeth and Leibold 2010, 2013, Firkowski et al. 2022). The documented spatial heterogeneity in experienced predation pressure from generalist mobile reef fishes across mat communities may significantly contribute to the maintenance of asynchrony in the dynamics of component communities in this cyanobacterial mat system via the creation of spatiotemporal complementarity in patterns of mat senescence (Fig 1b). The need to further understand and incorporate trophic interactions into our

understanding of mat metacommunity dynamics is critical, especially considering the increasingly dramatic environmental fluctuations experienced on reefs (i.e. massive pulse nutrient loadings; Firkowski et al. 2022). Trophic interactions may be a strong local-scale generator of asynchrony in community dynamics despite regional spatially synchronizing effects resulting from spatially correlated responses to environmental fluctuations driven by relatively low beta diversity among local mat communities (Cissell and McCoy in review), helping to maintain persistent mat cover at the scale of reef site. These data provide critical context toward explicitly incorporating trophic interaction strengths and variability into predictions of site and regional dynamics (Paine 1992, 2002).

The role of disturbance and the potential for top-down control

Disturbance events from both physical and biological processes are critical driving forces in the creation of spatiotemporal variability in the dynamics of natural communities (Sousa 1984). Indeed, local-scale interactions, including predator-prey linkages Livingston et al. 2017), are known to scale to the structure and function of entire communities and metacommunities (Baiser et al. 2013). Predatory interactions seem to be relevant mechanisms of disturbance for driving patterns across scales of organization in benthic cyanobacterial mats on coral reefs, from intra-mat scales (i.e. population-specific interactions from viral specialist predators [Fig. 5; Cissell and McCoy 2022a]), to whole community scales (i.e. generalist grazing from reef fishes [Fig. 3; Cissell et al. 2019]). Though strongly dependent upon the structure of the competitive network (Paine 1971), specialist predation is generally thought to have smaller direct effects on community and metacommunity stability (Howeth and Leibold 2010), which might suggest that predation from reef fishes on mats may play an outsized role over viral predation in driving

empirically observed community instability. We documented a diverse suite of grazers contributing to total mat community macropredatory pressure (Fig. 3). Because of differences in gape size and grazer physiology, significant differences in total foraging on mats among these different species of reef fishes suggests mats experience variability in both predation frequency and magnitude, which may in turn result in divergent physiological impacts to the mat intrinsically coupled to grazer identity (i.e., consumer trait-mediated effects).

Interestingly, VMR of the dominant cyanobacterial MAG in the *Living* sample was close to the natural diel variability of VMR associated with Cyanobacteria in other sampled mats from Bonaire, while the VMR in the *Decay* sample fell well above this diel spread (Cissell and McCoy 2022a). In other words, the dominant cyanobacterial population in the *Decay* sample had a greater abundance of viruses per capita than that experienced naturally by mat-building cyanobacteria across natural diel fluctuations. This offers further support that the viral abundances found in the *Decay* sample reflect true response to mat decay and suggest the potential for viral involvement in death and loss of mat structure, bolstered by the higher median relative abundance of all viruses in the community (Fig. 4), and shifts in the patterns (distribution) of the evenness structure of the viral community (Appendix S1: Figure S10). Higher viral activity in the *Border* sample (Fig. 4c) offers further evidence for active viral response to mat decay, and for heterogeneity in viral activity within mat communities. It should be pointed out, however, that these data are unable to resolve a causal link between viral predation and mat decay, as the exact timing of the viral increase cannot be inferred (i.e. we cannot differentiate viral causation vs. viral response to mat decay). Both viral lysis (Cohen 1949, Sillankorva et al. 2004) and lysogeny (Silveira et al. 2021) are known to be dependent upon host physiological state, which complicates predictions on causality vs response in this

system. Future work should expand on the evidence we present here on viral response to mat death toward explicitly uncovering spatially resolved patterns in viral infectivity within mat communities with increased replication at the level of mat and sampling location.

Microbial mats that form in other ecosystems are generally long-lived owing to their capabilities for nutrient recycling and retention (e.g. months - years; Doemel and Brock 1977, Bolhuis et al. 2014, Stal et al. 2019). Reef cyanobacterial mats possess similar mechanisms promoting nutrient retention within the mat system (Cissell and McCoy 2021; Cissell & McCoy in review), suggesting the feasibility of an *a priori* hypothesis predicting individual mat persistence on reefs and a minimization of the predominance of bottom-up control for mature mat community decay. This, in-turn, suggests that any observed patterns from dynamism in mat abundance should be primarily attributed to top-down forcing. This is not to say that bottom-up forcing does not influence mat growth dynamics, as bottom-up processes have long been implicated in mediating cyanobacterial mat growth rates (Kuffner and Paul 2001), but rather suggests that mat community dissolution and site-wide abundance of distinct mat individuals predominately responds to top-down forcing. The striking instability of mats that we have observed empirically over this relatively short time-period suggests that mat communities readily respond to top-down disturbance from predation. This might imply natural levels of predation experienced by mat communities impart strongly unidirectional outcomes on controlling mat communities, and is supported by the presence of a strong effect of top-down control in driving reductions of mat metacommunities in model simulations (Fig. 6).

The surprising outcomes from the field experimental coring (by suggesting non-linearity in the response of mat prey to predation pressure), however, complicate generalization of the role of top-down forcing in driving mat community dynamics. These experimental data, though, may

help to contextualize the relative magnitude of naturally occurring predation pressure. The nonequilibrium maintenance of biodiversity has long been thought to be dependent upon the frequency and magnitude of disturbance acting upon the system (Connell 1978). Indeed non-specific disturbance (including from generalist predators), in addition to density-dependent specialist predation (Paine 1971, Hewson et al. 2003, Thingstad et al. 2014), can be critical in the promotion of species coexistence by preventing competitive exclusion (Sousa 1979). Cyanobacterial mats are mutualistic consortia that depend upon metabolic coupling among physiologically and trophically distinct populations for community persistence (Cissell & McCoy in review). Maintenance of biodiversity, then, is critical for mat persistence, which would suggest some intermediate level of disturbance may benefit the longevity of individual mat communities. Indeed, maintenance of high intra-mat biodiversity likely stabilizes mean community productivity and buffers variability in critical community functions in the face of relatively stochastic but extreme-in-magnitude environmental fluctuations from anthropogenically-derived terrestrial-based nutrient subsidies (i.e. the insurance hypothesis; Yachi and Loreau 1999, Ford et al. 2017). Stabilizing interactions (both immediate and cascading from pulse restructuring of interaction networks [Fazzino et al. 2019]) from exogenous predation may further benefit mat longevity by buffering mat communities against the destabilizing effects of extensive cooperation (May 1972, Allesina and Tang 2012, Coyte et al. 2015). The significantly increased longevity of those mats in the experimental coring treatment qualitatively supports this biodiversity maintenance hypothesis (Fig. 2b) and suggests that natural predation regimes experienced by mats on the reefs in Bonaire may be on the low side of intermediate. This may at first appear counterintuitive to the outputs from the model simulations, which suggest that moderate predation pressure (including empirically informed levels of fish

predation) imparts significant mortality on mats and depreciation of metacommunity abundance, which would imply decreased longevity of component communities. However, importantly, these model simulations necessarily exclude the existence of interactive effects among trophic events and growth rate (independently estimated and not dynamic), and were limited in assuming homogeneity of predation risk across axes of time and space. This homogeneity applied even for high-in-magnitude low-in-frequency disturbance events arising from the foraging behavior of goatfishes. Indeed, the 'Low' predation model simulations imposed control over mat metacommunity abundance from saturating at 100%. In other words, the 'Medium' predation scenario in the model assumed homogeneity of pressure across both time and space, which may have pushed these modeled scenarios beyond what may be typically viewed as 'intermediate' levels of disturbance. Additionally, model outputs approximated cover estimates at the level of metacommunity, and did not track the dynamics of individual mat communities. In this way, the model more closely approximated the resolution of typical monitoring surveys, and cannot make inference on the ability of the different parameterizations of predation risk to entirely remove individual mat communities.

Generalized metabolic cooperation may also be predicted to be detrimental to community stability, however, by imposing an interdependence of population densities (May 1972, Allesina and Tang 2012, Coyte et al. 2015, Hoek et al. 2016). If top-down control disrupts cooperative interactions, especially asynchronously (Paine and Fenchel 1994), then metabolic cooperation may become a double-edged sword due to the repercussions of decoupled cooperative interactions. Macropredation pressure on mats is necessarily heterogenous across an individual mat community 'landscape', and we found evidence to support that micropredation from viruses, too, is heterogenous across a mat community. Predation, then, could change local-scale linkages

within mat communities, as is observed in experimental microbial metacommunities (Livingston et al. 2017) and synthetic metabolically-coupled microbial networks (Fazzino et al. 2019), interacting with niche-based processes to drive metabolic asynchrony and promoting overall community instability. Instances of mat death have been observed radiating out from apparent bite scars, suggesting the potential for dynamics to not be dependent on discrete trophic events but rather linked to emergent higher order effects from cascading trophic influence (Appendix S1: Figure S12). Within-mat patch dynamics could arise when space is opened from macropredation for recolonization (local-scale disturbance), which may interact with heterogeneity in predation frequency to promote intra-mat landscape mosaics of taxonomic and functional richness (Sousa 1979, Paine and Levin 1981; Appendix S1: Figure S13). Similar patchy patterns of diversity have previously been demonstrated in hot-springs cyanobacterial mats during recolonization following experimental disturbance (Ferris et al. 1996, 1997). Primary recolonization of bare substrate is likely predominantly pioneered by cyanobacterial species (Stal et al. 1985), likely shifting total mat stoichiometry in C:N:S via an apparent cyanobacterial bias.

Niche plasticity within cyanobacterial mat component populations, however, may dampen negative effects of stoichiometric shifts (Cissell & McCoy in review). Linkages among metabolic asynchrony, biodiversity maintenance, predation pressure, and community spatiotemporal asynchrony warrant further exploration across diverse systems with differing levels of predation pressure (i.e. varying biotic and abiotic context; Cissell et al. 2019, Ford et al. 2021, Ribeiro et al. 2022) to better understand the influence of predation in driving the structure and dynamics of cyanobacterial mat communities and metacommunities.

The rescuing role of dispersal

Our simulations predict that strong dispersal can meaningfully rescue mat metacommunities from extinction even under scenarios of strong top-down pressure and growth-limiting bottom-up control (Fig. 6). Dispersal may be especially crucial in supporting mat metacommunity persistence during episodic periods of relatively stable top-down pressure and strong bottom-up control in generally oligotrophic reef environments experiencing periodic land-based input (Brocke et al. 2015a, den Haan et al. 2016, Ford et al. 2017). The results of our theoretical model contribute to explaining the apparent decoupling of mat cover from targeted management actions tailored to increasing bottom-up control (i.e., limiting nutrient inputs) periodically observed (e.g., high documented high mat cover despite low nutrient loads and low Anthropogenic influence; Brocke et al. 2015a), as our results suggest that strong dispersal would facilitate this persistence at the metacommunity scale during periods of strong control on individual community persistence imposed by management practices (Fig. 6). Dispersal linkages were previously suggested to be present among cyanobacterial mat communities from molecular evidence demonstrating strong genomic conservation among spatially distinct mats (Cissell & McCoy in review). For cyanobacterial mats, predation, especially from mobile predators, may be an important mechanism promoting mat dispersal (Cissell et al. 2019). Predation by reef fishes has previously been suggested as an important vector of dispersal for endosymbiotic dinoflagellates of corals via grazing and subsequent fecal deposition (Grupstra et al. 2021), and consumer-mediated dispersal is more generally thought to be an important, yet understudied component of microbial community assembly and dynamics (Grupstra et al. 2022). In mats, foraging by reef fishes, and especially goatfishes, may also mechanically dislodge mats from the sediment surface into the water column to be dispersed via water movement, in addition to

potential dispersal via fecal deposition. Further work is needed to better understand mechanisms of cyanobacterial mat dispersal across reef landscapes, as well as the temporal scope of these rescuing effects (duration of strong control and maintenance of cover from dispersal linkages).

Taken all together, mats living at sediment surface may experience interesting and unique trade-offs. One side of the tradeoff could be likened to a pseudo-reversal of the paradox of enrichment (Rosenzweig 1971) – treating surface sediment as the enriched prey resource, then prey capitalization on increased resource availability (i.e. growing primarily at the surface) may directly lead to prey population collapse (reversal) from density-dependent predator response. In this sense, minimizing surface-sediment biomass available for opportunistic or targeting grazing would increase individual mat longevity. However, if predation is critical for mat dispersal, component community instability from predation may be necessary for long-term metacommunity persistence – suggesting mat dynamics may be more closely akin to the classic 'blinking lights' models of metapopulation ecology describing the dynamics of short-lived populations (Levins 1969).

Top-down vs. bottom-up control and the importance of scale

The focus on documenting the relative influence of top-down forcing on mat dynamics herein is not to ignore or minimize the empirically documented importance of bottom-up factors (primarily sediment-bound nutrient context), and physical factors more generally, in governing the dynamics of cyanobacterial mats on coral reefs (Kuffner and Paul 2001, Albert et al. 2005, Hallock 2005, Ahern et al. 2007, Brocke et al. 2015b, Tebbett et al. 2022). Indeed, many of the documented responses to top-down forcing likely interact with other highly relevant physical driving factors such as light availability, temperature, hydrodynamics, and sediment/intra-mat

redox conditions. Regional-scale disturbance from physical wave energy and general hydrodynamic turbulence on sediment topography (including scouring) have previously been suggested as important determinants of cyanobacterial mat distribution on coral reefs (Thacker and Paul 2001, Tebbett et al. 2022). The formation of sand ripples from water motion may altogether preclude mat formation, and disrupt patterns of persistence in mature mats, contributing to site-scale patterns in mat distribution and persistence. The opening of channels from local-scale top-down trophic events within the generally cohesive structural matrix binding mat communities may create areas more susceptible to physical disruption from water movement (from the formation of non-cohesive edges), which may interactively contribute to mat dynamism. Such trophic-mediated intra-mat channels may further alter redox conditions in the underlying sediment, as cover of reef cyanobacterial mats (Brocke et al. 2015a), and macrophyte cover more generally (Boros et al. 2011), are shown to have strong linkages with sediment redox potential. Shifting redox potential may strongly change the habit of physical mat manifestations and may drive mat communities deeper into the underlying sediment or promote the full disintegration of conspicuous mat structure from shifting nutrient settings.

Though light availability at the sediment surface would maximize cyanobacterial photosynthetic efficiency, living subsurface may confer some benefits as described above in addition to protection from exposure from ultraviolet radiation which may damage critical photosynthetic machinery (Garcia-Pichel and Bebout 1996). Further, mat size at the surface across its life-span is likely an emergent result of interactions among predation pressure, hydrodynamic setting, and benthic nutrient supply, with a likely positive covariance among areal extension and experienced predation pressure (primarily from reef fishes).

This discussion raises an additional interesting point concerning the manifestation of mat 'death' presented herein. Our assessment of mat death was reliant upon conspicuous manifestations that were observable to the naked eye (Appendix S1: Figure S3), namely the disappearance of conspicuous mat matrix from the surface sediment. The dynamics of mat community senescence contain inherent issues of scale-dependence. Metatranscriptomic evidence from transcription patterns of gene regions involved in photosynthesis for the dominant cyanobacterial MAGs recovered in this study suggests nuanced population-scale dynamism in response to mat decay (Appendix S1: Figure S14) despite eventual community death (Appendix S1: Figure S4). Specifically, we present preliminary evidence suggestive of competitive release of the less dominant cyanobacterial MAG, with qualitatively increased expression of photosynthesis gene regions in the *Decay* sample (Appendix S1: Figure S14), indicative of an increased physiological condition of this cyanobacterial population and a general decoupling of population-scale (i.e., intra-mat) and community-scale (i.e., whole mat) patterns and responses in mat senescence. Indeed, viable microbial cells may still be present from the mat community, but may not be visible or may have migrated subsurface. Surface vs. subsurface manifestations of mats may be likened to 'life-stages' of mats that are coupled to immediate abiotic and biotic context and history. Further exploration of cell integrity / viability associated with the disappearance of conspicuous surface level cyanobacterial mat biomass is necessary to resolve how closely the disappearance of conspicuous mat matrix can be associated with true 'death' of individual mat communities. Additional work should focus on this nested hierarchical decoupling of population vs. community. vs. metacommunity responses to mat senescence from both diversity (i.e., consequences on microbial beta and gamma diversity), and functional perspectives.

Collectively, these data indicate that both top-down and bottom-up forcing should be considered when constructing general frameworks toward understanding the dynamics of cyanobacterial mats on coral reefs, and that scale - both in ecological organization and physical space - likely matters when determining the relevance of trophic forcing directionality. Understanding how trophic dynamics interact with mat cover across scales is critical toward the creation of well-informed management strategies for controlling standing mat biomass, and for preventing the formation of new mat biomass on reefs (Cissell and McCoy 2022b).

Additional natural history observations

We join recent calls in advocating for the importance of understanding and documenting system-specific natural history in addition to applying generalizable theory toward holistically asking and contextualizing hypothesis-driven research (Travis 2020). Toward that end, what follows is a curated selection of relevant natural history observations made during our study period that further contextualize the patterns and processes presented herein, and which hopefully will generate and inform future hypotheses about relevant pattern-generating mechanisms in the dynamics of benthic cyanobacterial mat metacommunities.

In Bonaire, the foraging behavior of the goatfishes *M. martinicus* and *Ps. maculatus* can both directly and indirectly disturb benthic cyanobacterial mats. As a direct result of foraging in sediment underlying mats, *M. martinicus* individuals can disrupt mat structure, and remove sections of the mat from the benthos. This disturbance to mat biomass results primarily from the ‘shovel’ and ‘push’ feeding modes, however ‘skimming’ behavior also disrupts mat structure. These individuals are likely not foraging on the mat itself, as goatfish primarily forage on benthic invertebrates (Krajewski et al. 2006). Goatfish targeting of sediment underlying mats for forays

may be promoted by the forced vertical migration of sediment infauna toward the sediment surface from mat-promoted sediment anoxia (Brocke et al. 2015a), as previously suggested by Cissell et al. (2019) when discussing the targeting of mats by other mobile omnivorous reef fishes (primarily *Po. paru* [French Angelfish]). In addition to the direct effects of foraging on sediment underlying mats, we observed that *M. martinicus* individuals can partially or completely bury a mat in sediment by foraging nearby, as we directly observed (Appendix S1: Figure S15). Indirectly, this rapid sedimentation of mat surface area should negatively impact mat photosynthetic yield and efficiency – the dominant pathway of primary carbon acquisition in cyanobacterial mats (Cissell and McCoy 2021) – as is observed in other photosynthetic taxa (Izagirre et al. 2009). This would necessitate relatively rapid vertical migration of the mat structure to overcome the rapid sedimentation event, or rapid shifts in the predominance of enzymatic machinery, and could even disrupt carbon balances within mats.

On numerous occasions during our observational period, we observed *Elysia crispata* (Lettuce Sea Slug) individuals on benthic cyanobacterial mats overgrowing both hard substrate and sediment (Appendix S1: Figure S16). Although in this study we did not directly quantify consumption of mats by *E. crispata* individuals and so we cannot say how circumstantial these associations were, multiple lines of evidence suggest their ability and potential to consume benthic cyanobacterial mats. *E. crispata* are members of the Sacoglossa, marine sea slugs within the Opisthobranchia, and are specialist herbivores that feed on marine algae and seagrass (Clark and Busacca 1978). Many species within this group retain functional, diet-derived plastids in a process called kleptoplasty. This unique phenomenon is restricted in metazoans to members of this gastropod taxon. Among the Sacoglossa, the genus *Elysia* shows the most diverse range of organisms targeted, with *E. crispata* targeting a notably wide range of food organisms (Händeler

and Wägele 2007). Other Opisthobranchs (*Stylocheilus* spp.) are known specialist consumers of benthic cyanobacterial mats on both Caribbean (Capper and Paul 2008, Arthur et al. 2009) and Pacific coral reefs (Nagle et al. 1998). Furthermore, since *E. crispata* lack shells, benthic cyanobacterial mats may be a rich source of toxic secondary metabolites that these individuals could sequester and use to decrease their susceptibility to predation, which has been previously observed in Sacoglossans with noxious secondary metabolites derived from siphonalean green algae (Hay et al. 1989). Some Sacoglossans show ontogenetic shifts in dietary targets (Curtis et al. 2006), and therefore consumption of benthic cyanobacterial mats by *E. crispata* individuals may vary across its development. We recommend that future work be directed toward understanding the interactions between *E. crispata* and benthic cyanobacterial mats, including kleptoplasty, the assimilation of toxic secondary metabolites from the mat, and the level of disturbance the mat may sustain resulting from these potential interactions.

St. partitus (bicolor damselfish) individuals were found associated with 19 of the 22 cyanobacterial mats observed for fish foraging observations (~86%). During the observation periods, we observed numerous antagonistic chases against heterospecific grazers that resulted in predator deterrence from grazing with associational retention of the damselfish individual(s) near (often directly above) the conspicuous mat matrix throughout the entire observation period, suggesting these cyanobacterial mats fall within the territories of these *St. partitus* individuals (Myrberg 1972). These territories were not exclusive from conspecifics, however, with a maximum of three *St. partitus* individuals being observed simultaneously within frame over a single observed mat community (mean 1.8 individuals per mat community). Bites on mat communities by *St. partitus* individuals were quite frequent (Fig. 3) but were small in magnitude. Other damselfishes, including other species within the genus *Stegastes*, are well known for their

‘farming’ behavior with algal turfs – a mutualism that promotes algal growth via nutrient subsidies and protection from predators via behaviorally-mediated exclusion while the farming damselfish receives a consistent nutrient-dense food source (Hata et al. 2010, Blanchette et al. 2019). We hypothesize a similar relationship with emergent cyanobacterial mats falling within the territories of bicolor damselfish, which may contribute to the documented heterogeneity in predation pressure from reef fishes across component communities within a mat metacommunity, suggesting that the biotic context of cyanobacterial mats is likely a critical contributor to variability among individual mat community dynamics. Maintaining lawns consisting largely of benthic cyanobacterial mat cover may help increase nitrogen intake rates of *St. partitus* individuals given the relatively low C:N ratios of some mat-forming marine benthic cyanobacterial species relative to the upright filamentous algal species that are often farmed by damselfishes (Atkinson and Smith 1983, Hata and Kato 2002). Alternatively, the bites we observed during our video observations may represent individuals attempting to weed out and promote exclusion of these cyanobacterial mats from their territory in an attempt to maintain cover of non-cyanobacterial mat algal taxa (Hata and Kato 2004). Further work should attempt to differentiate among these competing behavioral hypotheses to better understand the relationship between farming damselfish and benthic cyanobacterial mats.

The immediate physical context of reef structure surrounding spatially distinct mat communities may play an outsized role in determining experienced predation pressure and driving variation in predation among mat communities. Structural complexity has long been thought to mediate the relative effects of competition vs. predation in driving community diversity (Menge and Sutherland 1976) by mediating predation intensity and interacting with foraging efficiency, preventing overexploitation (Paine 1974). These same arguments logically

extend to cyanobacterial mat communities from the perspective of both community diversity and biomass (links discussed in more detail above). The physical context also likely interacts with the maximal areal extent (i.e. by driving resource availability through shading and hydrodynamic disruption), which may be further interrelated with experienced predation pressure. In one instance during observations of fish foraging behavior associated with mats, we observed 494 bites taken on a single relatively unprotected (minimal surrounding physical structure) large-in-area benthic cyanobacterial mat during a time span of 26:05, dominated by bites from *Sc. iseri* individuals (255 and 108 bites from initial phase and terminal phase individuals respectively). This 'foraging frenzy' significantly disrupted a majority of the visible mat structural matrix. Interestingly, structural context has previously been hypothesized to mediate herbivorous pressure from reef fishes on basal trophic resources, though with increased herbivorous pressure with greater physical structure (Vergés et al. 2011). This implies that the spatial scale at which these relationships are measured (i.e. seascape vs. local) matter when relating physical context to predation risk. We suggest future research efforts focus on understanding how seascape-scale physical context contributes to heterogeneity in predation pressure experienced by cyanobacterial mat communities and overall temporal asynchrony in community dynamics.

Coral reef benthic cyanobacterial mats: A unifying definition

An explicit definition of coral reef benthic cyanobacterial mats as a functional grouping that clearly differentiates them from similar benthic functional groupings on reefs (e.g. epilithic algal matrix and tufting cyanobacterial assemblages) is critical for creating a unified framework toward their study moving forward. Here we leverage observations made during this study with previous observational and experimental work on benthic cyanobacterial mat communities to

propose a working definition of coral reef benthic cyanobacterial mats. Coral reef benthic cyanobacterial mats seem to be primarily horizontally-spreading (but can sometimes form vertical topography; Charpy et al. 2012), relatively short-lived (individual ephemerality; Fig. 1b), conspicuous benthic consortia primarily comprised of members of the phyla Cyanobacteria, Proteobacteria, and Bacteroidetes, with a distinct lack of a robust eukaryotic phototrophic assemblage (i.e. minimal relative abundance of diatoms and multicellular microbial algae; Cissell & McCoy 2021, Cissell & McCoy in review; though see Biessy et al. 2021). Composition among mats at a local scale (e.g. within reef site beta diversity) displays remarkably minimal heterogeneity (Cissell & McCoy in review). At higher taxonomic rankings, mat composition is also seemingly well-conserved across broader geographic ranges (Biessy et al. 2021), though biogeographic differences in the composition of the dominant cyanobacterial taxa in benthic mats have previously been proposed, mediated via local environmental context (Charpy et al. 2012b, Echenique-Subiabre et al. 2015). The taxonomic complexity of mats is complemented by a rich functional complexity encompassing both oxic and anoxic metabolisms, with ecophysiological and/or molecular evidence supporting mat contributions to the cycling of carbon, nitrogen, sulfur, and phosphorous on reefs (Charpy et al. 2007, 2010, Brocke et al. 2015b, 2018, den Haan et al. 2016, Cissell and McCoy 2021). Critically, facilitative interactions, primarily in the form of coupling of metabolic intermediates and localized detoxification of harmful sulfur and oxygen species (Cissell & McCoy in review), are important toward internal mat nutrient cycling and mat longevity. It is worth noting here that current methodologies toward resolving species interactions in complex microbial communities are inherently limited in their ability to precisely enumerate and decipher interaction strengths and nuanced ecological identities owing, in-part, to limitations in resolution (microdiversity), generating implicit rather

than explicit characterizations of interactions. Like other well-studied cyanobacterial mats (Stal 1995), members of the phylum Cyanobacteria likely provide the majority of the physical structure, binding together the mat matrix and pioneering novel mat structure on reef benthos. The larger size of cyanobacterial cells and filaments likely means the majority of cyanobacterial mat biomass and visible mat structure is dominated by members of the phylum Cyanobacteria despite not comprising an overwhelming dominance in sequencing space (relative shotgun sequencing abundance; Cissell & McCoy 2021, Cissell & McCoy in review). This abundance vs. biomass dominance has important implications for the nutritional quality of cyanobacterial mats as a foraging target to mobile predators (Clements et al. 2017, Cissell et al. 2019, Cissell and McCoy 2022b). Benthic cyanobacterial mats are competitive for space with other benthic taxa, and engage in active physiochemical competition with important reef building taxa such as scleractinian corals (Puyana et al. 2019). However, caging experiments provides evidence suggesting that benthic cyanobacterial mats are not competitively dominant over other benthic photosynthetic taxa such as important reef macroalgae (evidence specifically from *Dictyota bartayresiana*, *Padina tenuis*, and *Tolypiocladia glomerulata*; Thacker et al. 2001). This suggests that cyanobacterial members of mats, being primarily responsible for the colonization of bare space and extension of mat physical structure, are likely *r*-selected organisms and rapidly colonize bare benthos during periods of resource surplus (Andrews and Harris 1986). Indeed, microbial *r*-strategists are favored in ecosystems with fluctuating resource availability, such as coral reefs which receive pulses of land-based pollutants (Ford et al. 2017, Vadstein et al. 2018), and we directly observed cyanobacterial mats rapidly colonizing bare space created within an otherwise cohesive mat matrix on the order of hours (Appendix S1: Figure S13). In addition to those benefits presented herein (Fig. 2b), these previous caging experiments offer further

evidence toward potential benefits of macropredation pressure for cyanobacterial mat persistence, in this case, mediated via indirect effects on the competitive network topology similar to classic examples in competing intertidal coralline algal crusts (Paine 1984).

Synthesis and future recommendations

Here, we showed that coral reef benthic cyanobacterial mat metacommunities are temporally stable despite dramatic instability in component community patches across short time scales (Fig. 1). This decoupling of extinction risk across scales is likely linked to spatiotemporal asynchrony in the dynamics of component patches, which may be driven by heterogeneity in predation pressure both within (viruses; Fig. 4 & 5) and across (fishes; Fig. 3) communities. Predation pressure may not drive unidirectional outcomes in benthic cyanobacterial mat dynamics, though, with field experiments demonstrating a decreased instantaneous mortality rate of mats in response to increased predation pressure (Fig. 2b), potentially mediated via disturbance:diversity relationships. Dispersal may also play a strong role in driving the dynamics of mat metacommunities and is predicted in simulation modeling to confer a rescue effect to mat cover under scenarios of strong top-down and bottom-up control (Fig. 6). These data establish critical baselines and generate hypotheses relevant to ecologists and managers alike on the processes maintaining cyanobacterial dominance of coral reefs. We recommend that future work on cyanobacterial mat metacommunities focus increasingly on 1) explicitly understanding spatiotemporal variability in fluctuations among taxonomically (and, perhaps more interestingly, functionally) distinct populations within local communities and among similar populations within the broader metapopulation toward further parsing the implicit hierarchical variance structure across these distinct yet linked levels of ecological organization (sensu Wang and

Loreau 2014, Hammond et al. 2020); 2) identifying the relevant mechanisms and spatial structure of dispersal (as previously recommended in Cissell et al. 2022); 3) working toward understanding the link between the stability in metacommunity biomass reported here, and both the mean and spatiotemporal variance in mat metacommunity functional ecology (i.e., metacommunity scale DOC release, N_2 fixation, etc.; Brocke et al. 2015b, 2018, Cissell & McCoy in review); and 4) working toward quantifying the linkage strengths of trophic interrelations reported herein using classic removal experiments to further disentangle the importance of coupled dynamical trophic modules vs competitive linkages previously reported (Thacker et al. 2001, Puyana et al. 2019) in structuring benthic cyanobacterial mat metacommunity demography on coral reefs (Paine 1980).

ACKNOWLEDGMENTS

This work was supported by grants from the PADI Foundation (Grant Number: 40829), the Western Society of Naturalists (Rafe Sagarin Fund for Innovative Ecology), and the Phycological Society of America (Grant-In-Aid of Research) awarded to E.C. Cissell. Additional funding was provided by a gift from the Tatelbaum Fund and start-up funding from Florida State University to S.J. McCoy. E.C. Cissell was supported by a National Science Foundation Graduate Research Fellowship (Grant Number: 074012-520-044116) and a Mote Research Assistantship from the William R. and Lenore Mote Eminent Scholar in Marine Biology Endowment at Florida State University. We thank R.L. Francisca and C.E. Eckrich at Stichting Nationale Parken (STINAPA) Bonaire and Rijkswaterstaat Ministerie van Infrastructuur en Waterstaat for research permissions for conducting this work within the Bonaire National Marine Park. We extend our thanks to J.C. Manning, I. Basden, M. Dziewit, and B. Clark for assistance

in the field, and L. Kury in the analysis of benthic photoquadrat data. We thank A. Brown and the Florida State University Department of Biological Science Core Facility for help with molecular extractions and library preparation. We thank C. Peters for supporting the diving component of this work. We thank D.K. Okamoto for help with statistical analyses. Finally, we thank J.R. Cissell, K.M. Majzner, J.C. Manning, K.L. Dobson M. Huettel, D.K. Okamoto, K.M. Jones, and D.R. Rokyta for discussions and feedback on earlier versions of this manuscript.

AUTHOR CONTRIBUTIONS

E.C. Cissell conceived of and designed the study with significant contributions from S.J. McCoy. E.C. Cissell led all data collection in the field, and all in-situ data analyses and bioinformatics. S.J. McCoy significantly contributed to in-situ data analysis. E.C. Cissell drafted the original manuscript with significant contributions from S.J. McCoy. Both authors contributed significantly to manuscript revision.

CONFLICT OF INTEREST STATEMENT

The authors declare they have no known competing financial interests or personal relationships that did or could have appeared to influence the work reported in this paper.

REFERENCES

Ahern, K. S., C. R. Ahern, and J. W. Udy. 2007. Nutrient additions generate prolific growth of Lyngbya majuscula (cyanobacteria) in field and bioassay experiments. Harmful Algae 6:134–151.

Albert, S., J. M. O'Neil, J. W. Udy, K. S. Ahern, C. M. O'Sullivan, and W. C. Dennison. 2005. Blooms of the cyanobacterium Lyngbya majuscula in coastal Queensland, Australia: disparate sites, common factors. Marine Pollution Bulletin 51:428–437.

Allesina, S., and S. Tang. 2012. Stability criteria for complex ecosystems. Nature 483:205–208.

Andrews, J. H., and R. F. Harris. 1986. r-and K-selection and microbial ecology. Pages 99–147 Advances in microbial ecology. Springer.

Arthur, K., V. Paul, H. Paerl, J. O'Neil, J. Joyner, and T. Meickle. 2009. Effects of nutrient enrichment of the cyanobacterium Lyngbya sp. on growth, secondary metabolite concentration and feeding by the specialist grazer Stylocheilus striatus. Marine Ecology Progress Series 394:101–110.

Atkinson, M. J., and S. V. Smith. 1983. C:N:P ratios of benthic marine plants. Limnology and Oceanography 28:568–574.

Baiser, B., H. L. Buckley, N. J. Gotelli, and A. M. Ellison. 2013. Predicting food web structure with metacommunity models. Oikos 122:492–506.

Biessy, L., S. A. Wood, M. Chinain, M. Roué, and K. F. Smith. 2021. Exploring benthic cyanobacterial diversity and co-occurring potentially harmful dinoflagellates in six islands of the South Pacific. Hydrobiologia 848:2815–2829.

Blanchette, A., T. Ely, A. Zeko, S. A. Sura, R. Turba, and P. Fong. 2019. Damselfish Stegastes nigricans increase algal growth within their territories on shallow coral reefs via

enhanced nutrient supplies. Journal of Experimental Marine Biology and Ecology 513:21–26.

Bland, C., T. L. Ramsey, F. Sabree, M. Lowe, K. Brown, N. C. Kyrpides, and P. Hugenholtz. 2007. CRISPR Recognition Tool (CRT): a tool for automatic detection of clustered regularly interspaced palindromic repeats. BMC Bioinformatics 8:209.

Bolhuis, H., M. Silvia Cretoiu, and L. Stal. 2014. Molecular ecology of microbial mats. FEMS Microbiology Ecology.

Boros, G., M. Søndergaard, P. Takács, Á. Vári, and I. Tátrai. 2011. Influence of submerged macrophytes, temperature, and nutrient loading on the development of redox potential around the sediment–water interface in lakes. Hydrobiologia 665:117–127.

Brocke, H. J., B. Piltz, N. Herz, R. M. M. Abed, K. A. Palinska, U. John, J. den Haan, D. de Beer, and M. M. Nugues. 2018. Nitrogen fixation and diversity of benthic cyanobacterial mats on coral reefs in Curaçao. Coral Reefs 37:861–874.

Brocke, H. J., L. Polerecky, D. de Beer, M. Weber, J. Claudet, and M. M. Nugues. 2015a. Organic Matter Degradation Drives Benthic Cyanobacterial Mat Abundance on Caribbean Coral Reefs. PLOS ONE 10:e0125445.

Brocke, H. J., F. Wenzhoefer, D. de Beer, B. Mueller, F. C. van Duyl, and M. M. Nugues. 2015b. High dissolved organic carbon release by benthic cyanobacterial mats in a Caribbean reef ecosystem. Scientific Reports 5:8852.

Bruggemann, J. H., M. W. M. Kuyper, and A. M. Breeman. 1994b. Comparative analysis of foraging and habitat use by the sympatric Caribbean parrotfish Scarus vetula and Sparisoma viride (Scaridae). Marine Ecology Progress Series 112:51–66.

Capper, A., and V. J. Paul. 2008. Grazer interactions with four species of Lyngbya in southeast Florida. Harmful Algae 7:717–728.

Charpy, L., R. Alliod, M. Rodier, and S. Golubic. 2007. Benthic nitrogen fixation in the SW New Caledonia lagoon. Aquatic Microbial Ecology 47:73–81.

Charpy, L., B. E. Casareto, M. J. Langlade, and Y. Suzuki. 2012a. Cyanobacteria in Coral Reef Ecosystems: A Review. Journal of Marine Biology.

Charpy, L., K. A. Palinska, R. M. M. Abed, M. J. Langlade, and S. Golubic. 2012b. Factors influencing microbial mat composition, distribution and dinitrogen fixation in three western Indian Ocean coral reefs. European Journal of Phycology 47:51–66.

Charpy, L., K. A. Palinska, B. Casareto, M. J. Langlade, Y. Suzuki, R. M. M. Abed, and S. Golubic. 2010. Dinitrogen-Fixing Cyanobacteria in Microbial Mats of Two Shallow Coral Reef Ecosystems. Microbial Ecology 59:174–186.

Cissell, E. C., C. E. Eckrich, and S. J. McCoy. 2022. Cyanobacterial mats as benthic reservoirs and vectors for coral black band disease pathogens. Ecological Applications 32:e2692.

Cissell, E. C., J. C. Manning, and S. J. McCoy. 2019. Consumption of benthic cyanobacterial mats on a Caribbean coral reef. Scientific Reports 9:12693.

Cissell, E. C., and S. J. McCoy. 2021. Shotgun metagenomic sequencing reveals the full taxonomic, trophic, and functional diversity of a coral reef benthic cyanobacterial mat from Bonaire, Caribbean Netherlands. Science of The Total Environment 755:142719.

Cissell, E. C., and S. J. McCoy. 2022a. Top-heavy trophic structure within benthic viral dark matter. bioRxiv. https://doi.org/10.1101/2022.10.01.510451.

Cissell, E. C., and S. J. McCoy. 2022b. Marine cyanobacteria in the Anthropocene: Are top-down paradigms robust to climate change? Climate Change Ecology 3:100057.

Clark, K. B., and M. Busacca. 1978. Feeding specificity and chloroplast retention in four tropical ascoglossa, with a discussion of the extent of chloroplasts symbiosis and the evolution of the order. Journal of Molluscan Studies 44:272–282.

Clements, K. D., D. German, J. Piché, A. Tribollet, and J. H. Choat. 2017. Integrating ecological roles and trophic diversification on coral reefs: multiple lines of evidence identify parrotfishes as microphages. Biological Journal of the Linnean Society 120:729–751.

Cohen, S. 1949. Growth requirements of bacterial viruses. Bacteriology Reviews 13:1–24.

Connell, J. H. 1978. Diversity in tropical rain forests and coral reefs: high diversity of trees and corals is maintained only in a nonequilibrium state. Science 199:1302–1310.

Connell, J. H., T. P. Hughes, and C. C. Wallace. 1997. A 30 year study of coral abundance, recruitment, and disturbance at several scales in space and time. Ecological Monographs 67:461–488.

Coutinho, F. H., C. B. Silveira, G. B. Gregoracci, C. C. Thompson, R. A. Edwards, C. P. D. Brussaard, B. E. Dutilh, and F. L. Thompson. 2017. Marine viruses discovered via metagenomics shed light on viral strategies throughout the oceans. Nature Communications 8:15955.

Coyte, K. Z., J. Schluter, and K. R. Foster. 2015. The ecology of the microbiome: networks, competition, and stability. Science 350:663–666.

Crowley, P. H. 1978. Effective size and the persistence of ecosystems. Oecologia 35:185–195.

Curtis, N. E., S. E. Massey, and S. K. Pierce. 2006. The symbiotic chloroplasts in the sacoglossan Elysia clarki are from several algal species. Invertebrate Biology 125:336–345.

Doemel, W. N., and T. D. Brock. 1977. Structure, Growth, and Decomposition of Laminated Algal-Bacterial Mats in Alkaline Hot Springs. Applied and Environmental Microbiology 34:433–452.

Echenique-Subiabre, I., A. Villeneuve, S. Golubic, J. Turquet, J.-F. Humbert, and M. Gugger. 2015. Influence of local and global environmental parameters on the composition of cyanobacterial mats in a tropical lagoon. Microbial Ecology 69:234–244.

Edwards, R. A., K. McNair, K. Faust, J. Raes, and B. E. Dutilh. 2016. Computational approaches to predict bacteriophage–host relationships. FEMS Microbiology Reviews 40:258–272.

Eren, A. M., Ö. C. Esen, C. Quince, J. H. Vineis, H. G. Morrison, M. L. Sogin, and T. O. Delmont. 2015. Anvi'o: an advanced analysis and visualization platform for 'omics data. PeerJ 3:e1319.

Falkenberg, L. J., B. D. Russell, and S. D. Connell. 2013. Future herbivory: the indirect effects of enriched CO2 may rival its direct effects. Marine Ecology Progress Series 492:85–95.

Fazzino, L., J. Anisman, J. M. Chacón, R. H. Heineman, and W. R. Harcombe. 2019. Lytic bacteriophage have diverse indirect effects in a synthetic cross-feeding community. The ISME Journal.

Fenchel, T. 1998. Formation of laminated cyanobacterial mats in the absence of benthic fauna. Aquatic Microbial Ecology 14:235–240.

Ferris, M. J., S. C. Nold, N. P. Revsbech, and D. M. Ward. 1997. Population structure and physiological changes within a hot spring microbial mat community following disturbance. Applied and Environmental Microbiology 63:1367–1374.

Ferris, M., A. Ruff-Roberts, E. Kopczynski, M. Bateson, and D. Ward. 1996. Enrichment culture and microscopy conceal diverse thermophilic Synechococcus populations in a single hot spring microbial mat habitat. Applied and Environmental Microbiology 62:1045–1050.

Firkowski, C. R., P. L. Thompson, A. Gonzalez, M. W. Cadotte, and M. Fortin. 2022. Multi□trophic metacommunity interactions mediate asynchrony and stability in fluctuating environments. Ecological Monographs 92:e01484.

Ford, A. K., S. Bejarano, M. M. Nugues, P. M. Visser, S. Albert, and S. C. A. Ferse. 2018. Reefs under Siege—the Rise, Putative Drivers, and Consequences of Benthic Cyanobacterial Mats. Frontiers in Marine Science 5:18.

Ford, A. K., N. Van Hoytema, B. R. Moore, L. Pandihau, C. Wild, and S. C. A. Ferse. 2017. High sedimentary oxygen consumption indicates that sewage input from small islands drives benthic community shifts on overfished reefs. Environmental Conservation 44:405–411.

Ford, A. K., P. M. Visser, M. J. van Herk, E. Jongepier, and V. Bonito. 2021. First insights into the impacts of benthic cyanobacterial mats on fish herbivory functions on a nearshore coral reef. Scientific Reports 11:7147.

Garcia-Pichel, F., and B. Bebout. 1996. Penetration of ultraviolet radiation into shallow water sediments:high exposure for photosynthetic communities. Marine Ecology Progress Series 131:257–262.

Grupstra, C. G. B., K. M. Rabbitt, L. I. Howe-Kerr, and A. M. S. Correa. 2021. Fish predation on corals promotes the dispersal of coral symbionts. Animal Microbiome 3:25.

Grupstra, C., N. Lemoine, C. Cook, and A. Correa. 2022. Thank you for biting: dispersal of beneficial microbiota through’antagonistic’interactions. Trends in Microbiology.

Guo, J., B. Bolduc, A. A. Zayed, A. Varsani, G. Dominguez-Huerta, T. O. Delmont, A. A. Pratama, M. C. Gazitúa, D. Vik, M. B. Sullivan, and S. Roux. 2021. VirSorter2: a multi-classifier, expert-guided approach to detect diverse DNA and RNA viruses. Microbiome 9:37.

Guo, J., D. Vik, A. Adjie Pratama, S. Roux, and M. Sullivan. (n.d.). Viral sequence identification SOP with VirSorter2 v3.

Gurevich, A., V. Saveliev, N. Vyahhi, and G. Tesler. 2013. QUAST: quality assessment tool for genome assemblies. Bioinformatics 29:1072–1075.

den Haan, J., J. Huisman, H. J. Brocke, H. Goehlich, K. R. W. Latijnhouwers, S. van Heeringen, S. A. S. Honcoop, T. E. Bleyenberg, S. Schouten, C. Cerli, L. Hoitinga, M. J. A. Vermeij, and P. M. Visser. 2016. Nitrogen and phosphorus uptake rates of different species from a coral reef community after a nutrient pulse. Scientific Reports 6:28821.

Hallock, P. 2005. Global change and modern coral reefs: New opportunities to understand shallow-water carbonate depositional processes. Sedimentary Geology 175:19–33.

Hammond, M., M. Loreau, C. Mazancourt, and J. Kolasa. 2020. Disentangling local, metapopulation, and cross□community sources of stabilization and asynchrony in metacommunities. Ecosphere 11.

Händeler, K., and H. Wägele. 2007. Preliminary study on molecular phylogeny of Sacoglossa and a compilation of their food organisms. Bonner zoologische Beiträge:231–254.

Hata, H., and M. Kato. 2002. Weeding by the herbivorous damselfish Stegastes nigricans in nearly monocultural algae farms. Marine Ecology Progress Series 237:227–231.

Hata, H., and M. Kato. 2004. Monoculture and mixed-species algal farms on a coral reef are maintained through intensive and extensive management by damselfishes. Journal of Experimental Marine Biology and Ecology 313:285–296.

Hata, H., K. Watanabe, and M. Kato. 2010. Geographic variation in the damselfish-red alga cultivation mutualism in the Indo-West Pacific. BMC Evolutionary Biology 10:185.

Hay, M. E., J. R. Pawlik, J. E. Duffy, and W. Fenical. 1989. Seaweed-herbivore-predator interactions: host-plant specialization reduces predation on small herbivores. Oecologia 81:418–427.

van Heuzen, H. 2015. Occurrence of deep water Cyanobacterial Mats surrounding Bonaire.

Hewson, I., J. M. O[1]Neil, and W. C. Dennison. 2001. Virus-like particles associated with Lyngbya majuscula (Cyanophyta; Oscillatoriacea) bloom decline in Moreton Bay, Australia. Aquatic Microbial Ecology 25:207–213.

Hewson, I., G. A. Vargo, and J. A. Fuhrman. 2003. Bacterial Diversity in Shallow Oligotrophic Marine Benthos and Overlying Waters: Effects of Virus Infection, Containment, and Nutrient Enrichment. Microbial Ecology 46:322–336.

Hoek, T. A., K. Axelrod, T. Biancalani, E. A. Yurtsev, J. Liu, and J. Gore. 2016. Resource availability modulates the cooperative and competitive nature of a microbial cross-feeding mutualism. PLoS biology 14:e1002540.

Holyoak, M., and S. P. Lawler. 1996. Persistence of an extinction-prone predator-prey interaction through metapopulation dynamics. Ecology 77:1867–1879.

Howeth, J. G., and M. A. Leibold. 2010. Species dispersal rates alter diversity and ecosystem stability in pond metacommunities. Ecology 91:2727–2741.

Howeth, J. G., and M. A. Leibold. 2013. Predation inhibits the positive effect of dispersal on intraspecific and interspecific synchrony in pond metacommunities. Ecology 94:2220–2228.

Huisman, J., G. A. Codd, H. W. Paerl, B. W. Ibelings, J. M. H. Verspagen, and P. M. Visser. 2018. Cyanobacterial blooms. Nature Reviews Microbiology 16:471–483.

Hunter, M. D., and P. W. Price. 1992. Playing Chutes and Ladders: Heterogeneity and the Relative Roles of Bottom-Up and Top- Down Forces in Natural Communities. Ecology 73:724–732.

Hyatt, D., G.-L. Chen, P. F. LoCascio, M. L. Land, F. W. Larimer, and L. J. Hauser. 2010. Prodigal: prokaryotic gene recognition and translation initiation site identification. BMC Bioinformatics 11:119.

Izagirre, O., A. Serra, H. Guasch, and A. Elosegi. 2009. Effects of sediment deposition on periphytic biomass, photosynthetic activity and algal community structure. Science of The Total Environment 407:5694–5700.

Jain, C., L. M. Rodriguez-R, A. M. Phillippy, K. T. Konstantinidis, and S. Aluru. 2018. High throughput ANI analysis of 90K prokaryotic genomes reveals clear species boundaries. Nature Communications 9:5114.

Kang, D. D., F. Li, E. Kirton, A. Thomas, R. Egan, H. An, and Z. Wang. 2019. MetaBAT 2: an adaptive binning algorithm for robust and efficient genome reconstruction from metagenome assemblies. PeerJ 7:e7359.

Kieft, K., Z. Zhou, and K. Anantharaman. 2020. VIBRANT: automated recovery, annotation and curation of microbial viruses, and evaluation of viral community function from genomic sequences. Microbiome 8:90.

Kopylova, E., L. Noé, and H. Touzet. 2012. SortMeRNA: fast and accurate filtering of ribosomal RNAs in metatranscriptomic data. Bioinformatics 28:3211–3217.

Krajewski, J. P., R. M. Bonaldo, C. Sazima, and I. Sazima. 2006. Foraging activity and behaviour of two goatfish species (Perciformes: Mullidae) at Fernando de Noronha Archipelago, tropical West Atlantic. Environmental Biology of Fishes 77:1–8.

Kuffner, I., and V. Paul. 2001. Effects of nitrate, phosphate and iron on the growth of macroalgae and benthic cyanobacteria from Cocos Lagoon, Guam. Marine Ecology Progress Series 222:63–72.

Langmead, B., and S. L. Salzberg. 2012. Fast gapped-read alignment with Bowtie 2. Nature Methods 9:357–359.

Leibold, M. A., M. Holyoak, N. Mouquet, P. Amarasekare, J. M. Chase, M. F. Hoopes, R. D. Holt, J. B. Shurin, R. Law, and D. Tilman. 2004. The metacommunity concept: a framework for multi□scale community ecology. Ecology letters 7:601–613.

Levin, S. A. 1992. The problem of pattern and scale in ecology: the Robert H. MacArthur award lecture. Ecology 73:1943–1967.

Levins, R. 1969. Some demographic and genetic consequences of environmental heterogeneity for biological control. American Entomologist 15:237–240.

Li, H. 2013. Aligning sequence reads, clone sequences and assembly contigs with BWA-MEM. arXiv:1303.3997 [q-bio].

Li, W., and A. Godzik. 2006. Cd-hit: a fast program for clustering and comparing large sets of protein or nucleotide sequences. Bioinformatics 22:1658–1659.

Li, Z., D. Pan, G. Wei, W. Pi, C. Zhang, J.-H. Wang, Y. Peng, L. Zhang, Y. Wang, C. R. J. Hubert, and X. Dong. 2021. Deep sea sediments associated with cold seeps are a subsurface reservoir of viral diversity. The ISME Journal.

Livingston, G., K. Fukumori, D. B. Provete, M. Kawachi, N. Takamura, and M. A. Leibold. 2017. Predators regulate prey species sorting and spatial distribution in microbial landscapes. Journal of Animal Ecology 86:501–510.

May, R. M. 1972. Will a large complex system be stable? Nature 238:413–414.

McCoy, S. J., S. Allesina, and C. A. Pfister. 2016. Ocean acidification affects competition for space: projections of community structure using cellular automata. Proceedings of the Royal Society B: Biological Sciences 283:20152561.

McCoy, S. J., and N. A. Kamenos. 2018. Coralline algal skeletal mineralogy affects grazer impacts. Global change biology 24:4775–4783.

McCoy, S. J., N. A. Kamenos, P. Chung, T. J. Wootton, and C. A. Pfister. 2018. A mineralogical record of ocean change: Decadal and centennial patterns in the California mussel. Global Change Biology 24:2554–2562.

McCoy, S. J., and C. A. Pfister. 2014. Historical comparisons reveal altered competitive interactions in a guild of crustose coralline algae. Ecology Letters 17:475–483.

Menge, B. A., and J. P. Sutherland. 1976. Species Diversity Gradients: Synthesis of the Roles of Predation, Competition, and Temporal Heterogeneity. The American Naturalist 110:351–369.

Myrberg, A. A. 1972. Social Dominance and Territoriality in the Bicolor Damselfish, Eupomacentrus partitus (Poey) (Pisces□: Pomacentridae). Behaviour 41:207–230.

Nagle, D. G., F. T. Camacho, and V. J. Paul. 1998. Dietary preferences of the opisthobranch mollusc Stylocheilus longicauda for secondary metabolites produced by the tropical cyanobacterium Lyngbya majuscula. Marine Biology 132:267–273.

Nayfach, S., A. P. Camargo, F. Schulz, E. Eloe-Fadrosh, S. Roux, and N. C. Kyrpides. 2021. CheckV assesses the quality and completeness of metagenome-assembled viral genomes. Nature Biotechnology 39:578–585.

Nissen, J. N., J. Johansen, R. L. Allesøe, C. K. Sønderby, J. J. A. Armenteros, C. H. Grønbech, L. J. Jensen, H. B. Nielsen, T. N. Petersen, O. Winther, and S. Rasmussen. 2021. Improved metagenome binning and assembly using deep variational autoencoders. Nature Biotechnology.

Olm, M. R., C. T. Brown, B. Brooks, and J. F. Banfield. 2017. dRep: a tool for fast and accurate genomic comparisons that enables improved genome recovery from metagenomes through de-replication. The ISME Journal 11:2864–2868.

Paine, R. T. 1966. Food Web Complexity and Species Diversity. The American Naturalist 100:65–75.

Paine, R. T. 1971. A Short-Term Experimental Investigation of Resource Partitioning in a New Zealand Rocky Intertidal Habitat. Ecology 52:1096–1106.

Paine, R. T. 1974. Intertidal Community Structure. Experimental Studies on the Relationship between a Dominant Competitor and Its Principal Predator. Oecologia 15:93–120.

Paine, R. T. 1980. Food Webs: Linkage, Interaction Strength and Community Infrastructure. The Journal of Animal Ecology 49:666.

Paine, R. T. 1984. Ecological Determinism in the Competition for Space: The Robert H. MacArthur Award Lecture. Ecology 65:1339–1348.

Paine, R. T. 1992. Food-web analysis through field measurement of per capita interaction strength. Nature 355:73–75.

Paine, R. T. 2002. Trophic Control of Production in a Rocky Intertidal Community. Science 296:736–739.

Paine, R. T., and T. Fenchel. 1994. Marine rocky shores and community ecology: an experimentalist's perspective. Ecology Institute Oldendorf/Luhe, Germany.

Paine, R. T., and S. A. Levin. 1981. Intertidal Landscapes: Disturbance and the Dynamics of Pattern. Ecological Monographs 51:145–178.

Peng, Y., H. C. M. Leung, S. M. Yiu, and F. Y. L. Chin. 2012. IDBA-UD: a de novo assembler for single-cell and metagenomic sequencing data with highly uneven depth. Bioinformatics 28:1420–1428.

Petchey, O. L., P. T. McPhearson, T. M. Casey, and P. J. Morin. 1999. Environmental warming alters food-web structure and ecosystem function. Nature 402:69–72.

Power, M. E. 1992. Top-Down and Bottom-Up Forces in Food Webs: Do Plants Have Primacy. Ecology 73:733–746.

Puyana, M., J. A. Prato, C. F. Nieto, F. A. Ramos, L. Castellanos, P. Pinzón, and J. C. Zárate. 2019. Experimental Approaches for the Evaluation of Allelopathic Interactions Between Hermatypic Corals and Marine Benthic Cyanobacteria in the Colombian Caribbean. Acta Biológica Colombiana 24:243–254.

Quinn, T. P., I. Erb, G. Gloor, C. Notredame, M. F. Richardson, and T. M. Crowley. 2019. A field guide for the compositional analysis of any-omics data. GigaScience 8:giz107.

Reverter, M., M. Jackson, N. Daraghmeh, C. von Mach, and N. Milton. 2020. 11-yr of coral community dynamics in reefs around Dahab (Gulf of Aqaba, Red Sea): the collapse of urchins and rise of macroalgae and cyanobacterial mats. Coral Reefs.

Ribeiro, F. de V., T. A. Caires, M. A. de A. Simões, P. I. Hargreaves, L. B. Villela, G. de O. Fistarol, A. B. Caselgrandi, G. H. Pereira-Filho, R. L. de Moura, R. C. Pereira, and P. S. Salomon. 2022. Benthic Cyanobacterial Diversity and Antagonistic Interactions in Abrolhos Bank: Allelopathy, Susceptibility to Herbivory, and Toxicity. Frontiers in Marine Science 8:790277.

Ritson-Williams, R., V. J. Paul, and V. Bonito. 2005. Marine benthic cyanobacteria overgrow coral reef organisms. Coral Reefs 24:629–629.

Rodriguez-R, L. M., S. Gunturu, J. M. Tiedje, J. R. Cole, and K. T. Konstantinidis. 2018. Nonpareil 3: Fast Estimation of Metagenomic Coverage and Sequence Diversity. mSystems 3:e00039-18, /msystems/3/3/msys.00039-18.atom.

Rosenzweig, M. L. 1971. Paradox of Enrichment: Destabilization of Exploitation Ecosystems in Ecological Time. Science 171:385–387.

Sellanes, J., M. Gorny, G. Zapata-Hernández, G. Alvarez, P. Muñoz, and F. Tala. 2021. A new threat to local marine biodiversity: filamentous mats proliferating at mesophotic depths off Rapa Nui. PeerJ 9:e12052.

Shaffer, M., M. A. Borton, B. B. McGivern, A. A. Zayed, S. L. La Rosa, L. M. Solden, P. Liu, A. B. Narrowe, J. Rodríguez-Ramos, B. Bolduc, M. C. Gazitúa, R. A. Daly, G. J. Smith, D. R. Vik, P. B. Pope, M. B. Sullivan, S. Roux, and K. C. Wrighton. 2020. DRAM for distilling microbial metabolism to automate the curation of microbiome function. Nucleic Acids Research 48:8883–8900.

Sieber, C. M. K., A. J. Probst, A. Sharrar, B. C. Thomas, M. Hess, S. G. Tringe, and J. F. Banfield. 2018. Recovery of genomes from metagenomes via a dereplication, aggregation and scoring strategy. Nature Microbiology 3:836–843.

Sillankorva, S., R. Oliveira, M. J. Vieira, I. Sutherland, and J. Azeredo. 2004. *Pseudomonas fluorescens* infection by bacteriophage Î¦S1: the influence of temperature, host growth phase and media. FEMS Microbiology Letters 241:13–20.

Silveira, C. B., A. Luque, and F. Rohwer. 2021. The landscape of lysogeny across microbial community density, diversity and energetics. Environmental Microbiology 23:4098–4111.

Silverman, J. D., K. Roche, S. Mukherjee, and L. A. David. 2020. Naught all zeros in sequence count data are the same. Computational and structural biotechnology journal 18:2789–2798.

Sousa, W. P. 1979. Disturbance in Marine Intertidal Boulder Fields: The Nonequilibrium Maintenance of Species Diversity. Ecology 60:1225–1239.

Stal, L. J. 1995. Tansley Review No. 84 Physiological ecology of cyanobacteria in microbial mats and other communities. New Phytologist 131:1–32.

Stal, L. J., H. Bolhuis, and M. S. Cretoiu. 2019. Phototrophic marine benthic microbiomes: the ecophysiology of these biological entities. Environmental Microbiology 21:1529–1551.

Stal, L. J., H. Gemerden, and W. E. Krumbein. 1985. Structure and development of a benthic marine microbial mat. FEMS Microbiology Letters 31:111–125.

Tebbett, S. B., R. P. Streit, J. Morais, J. A. Schlaefer, S. Swan, and D. R. Bellwood. 2022. Benthic cyanobacterial mat formation during severe coral bleaching at Lizard Island: The mediating role of water currents. Marine Environmental Research:105752.

Thacker, R., D. Ginsburg, and V. Paul. 2001. Effects of herbivore exclusion and nutrient enrichment on coral reef macroalgae and cyanobacteria. Coral Reefs 19:318–329.

Thacker, R. W., and V. J. Paul. 2001. Are benthic cyanobacteria indicators of nutrient enrichment? Relationship between cyanobacterial abundance and environmental factors on the reef flats of Guam. Bulletin of Marine Science 69:12.

Thingstad, T. F., S. Vage, J. E. Storesund, R.-A. Sandaa, and J. Giske. 2014. A theoretical analysis of how strain-specific viruses can control microbial species diversity. Proceedings of the National Academy of Sciences 111:7813–7818.

Travis, J. 2020. Where Is Natural History in Ecological, Evolutionary, and Behavioral Science? The American Naturalist 196:1–8.

Vadstein, O., K. J. Attramadal, I. Bakke, and Y. Olsen. 2018. K-selection as microbial community management strategy: a method for improved viability of larvae in aquaculture. Frontiers in Microbiology 9:2730.

Vergés, A., M. A. Vanderklift, C. Doropoulos, and G. A. Hyndes. 2011. Spatial Patterns in Herbivory on a Coral Reef Are Influenced by Structural Complexity but Not by Algal Traits. PLOS ONE 6:e17115.

Wagner, G. P., K. Kin, and V. J. Lynch. 2012. Measurement of mRNA abundance using RNA-seq data: RPKM measure is inconsistent among samples. Theory in Biosciences 131:281–285.

Wang, S., and M. Loreau. 2014. Ecosystem stability in space: α, β and γ variability. Ecology letters 17:891–901.

Wilcox, K. R., A. T. Tredennick, S. E. Koerner, E. Grman, L. M. Hallett, M. L. Avolio, K. J. La Pierre, G. R. Houseman, F. Isbell, and D. S. Johnson. 2017. Asynchrony among local

communities stabilises ecosystem function of metacommunities. Ecology letters 20:1534–1545.

Wootton, J. T. 1993. Indirect Effects and Habitat Use in an Intertidal Community: Interaction Chains and Interaction Modifications. The American Naturalist 141:71–89.

Wu, Y.-W., B. A. Simmons, and S. W. Singer. 2016. MaxBin 2.0: an automated binning algorithm to recover genomes from multiple metagenomic datasets. Bioinformatics 32:605–607.

Yachi, S., and M. Loreau. 1999. Biodiversity and ecosystem productivity in a fluctuating environment: the insurance hypothesis. Proceedings of the National Academy of Sciences 96:1463–1468.

Zielezinski, A., S. Deorowicz, and A. Gudyś. 2022. PHIST: fast and accurate prediction of prokaryotic hosts from metagenomic viral sequences. Bioinformatics 38:1447–1449.

FIGURE CAPTIONS:

Figure 1. a, Barplots of site-scale proportional cover of cyanobacterial mats across sampling dates. Error bars correspond to standard error around the mean for each sampling date. Horizontal dashed line denotes mean cover across sampling dates. b, Line plot of cumulative percent of component communities dead across sampling dates. Rug barplots show individual mat death counts across dates (scaling axis not shown).

Figure 2. a, Probability of individual community death by treatment inclusion. Large circles denote mean probability of a mat community dying in each treatment; error bars represent SE. Individual points are binomial outcomes corresponding to if a mat died during the study period (0) or not (1). b, Exponential survival curves from benthic cyanobacterial mats subject to natural grazing pressure (Unmanipulated [U]; gray) vs mats experimentally wounded (Wounded [W]; pink) demonstrating reduction in instantaneous mortality rate with increased predation. Raw points (jittered vertically) show individual mat outcomes (binomial; 1=survival, 0=death).

Figure 3. Boxplots of bite count (#) by fish species. Data for *Ps. maculatus* and *M. martinicus* represent total number of forays that disturbed cyanobacterial mat biomass and not bites (see Section 5.2. Materials & Methods). *TP* and *IP* designation next to species names on y-axis denote *Terminal Phase* and *Initial Phase* respectively. Colors and silhouettes broadly group species by taxonomic family (i.e. Mullidae, Pomacanthidae, Acanthuridae, Scaridae, Pomacentridae from top to bottom). Fish silhouettes are from *R::fishualize*.

Figure 4. Violin plots of viral abundance (log_{10} transformed CPM normalized abundances) and viral activity (log_{10} transformed TPM normalized abundances) across samples. a, Rasterized (classified; mat area in black, sediment in white) image of sampled dying cyanobacterial mat showing actual points of sampling and broad areal classification (*Living* vs. *Border* vs. *Decay*) on mat area. Colors denote sample membership. Horizontal lines on violins denote the lower, median, and upper quartile. Points show abundance of individual vOTUs. Violin plots are grouped by patterns in abundance (b; from DNA) and activity (c; from RNA).

Figure 5. Population-resolved (from MAGs) Cyanobacteria:cyanophage dynamics. a, Sample-specific log_{10}-transformed VMR per recovered cyanobacterial MAG. b, Sample-specific relative abundance (log_{10} transformed CPM normalized counts) of both recovered cyanobacterial MAGs (circles), and host linked cyanophages (triangles). c, Sample-specific log_{10}-transformed VMAR per recovered cyanobacterial MAG. b, Sample-specific relative activity (log_{10} transformed TPM normalized counts) of both recovered cyanobacterial MAGs (circles), and host linked cyanophages (triangles). Colors encode distinct cyanobacterial MAG. Lines are not predictions from statistical regression; lines are given to aid in visual interpretation of trends.

Figure 6. Outputs from model simulations showing mean (from n=100 separate model simulations each) trajectory of cyanobacterial mat cover across the 1.25km^2 model grid area over 365 days. Plots are faceted by different parameterizations of growth rate across the X axis, and different parameterizations of predation rate across the Y axis. Different parameterizations of dispersal rate are encoded in different line colors. Lines do not represent statistical regressions, and are present to aid in trend visualization.

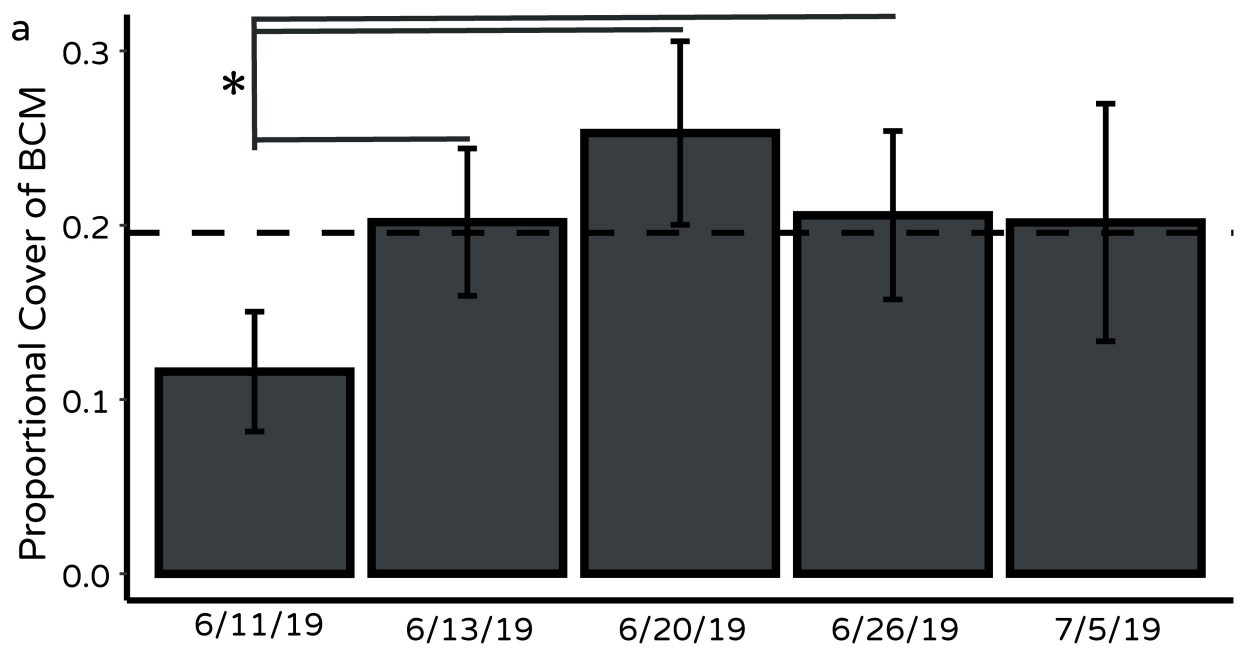
a
Proportional Cover of BCM
0.3
0.2
0.1
0.0
*
6/11/19
6/13/19
6/20/19
6/26/19
7/5/19

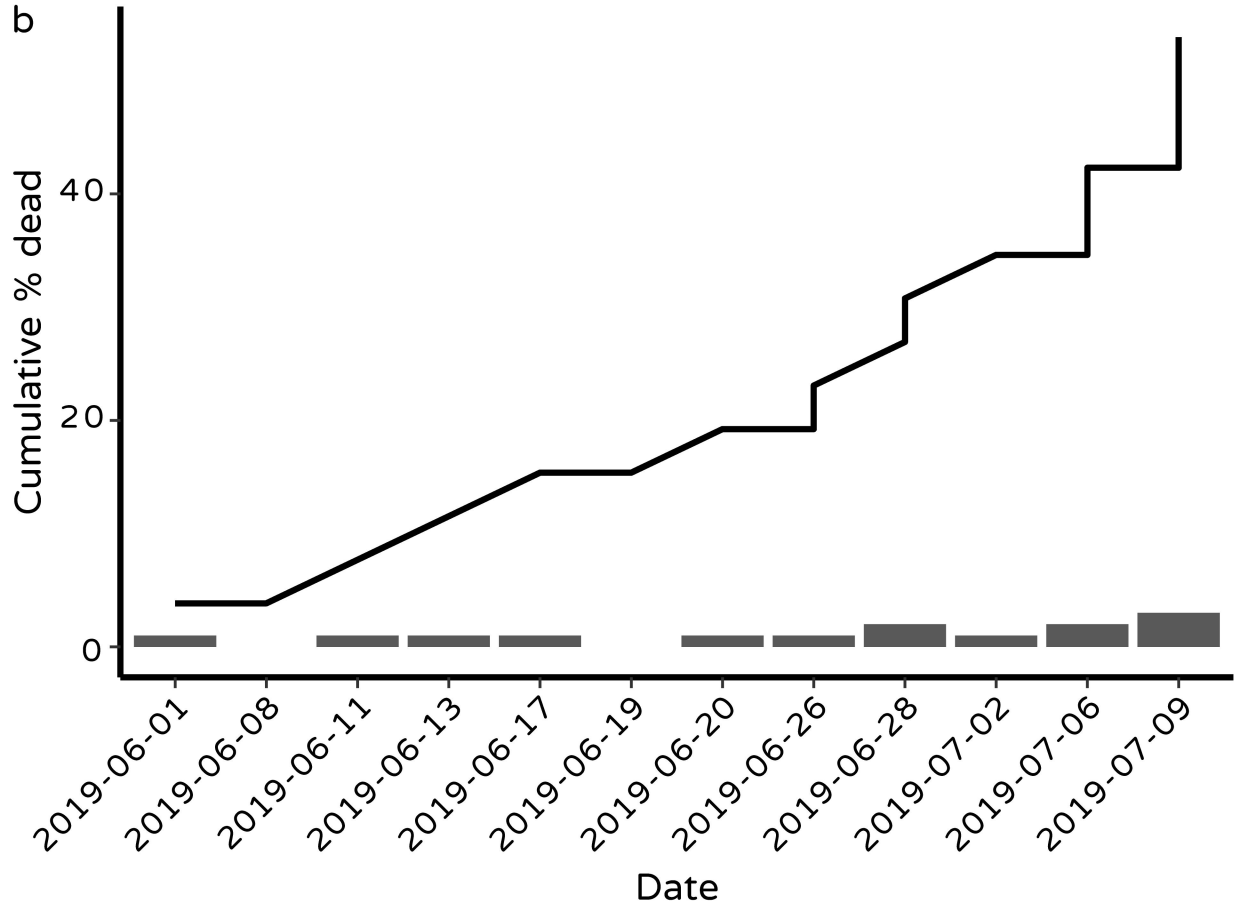
b
Cumulative % dead
40
20
0
2019-06-01
2019-06-08
2019-06-11
2019-06-13
2019-06-17
2019-06-19
2019-06-20
2019-06-26
2019-06-28
2019-07-02
2019-07-06
2019-07-09
Date

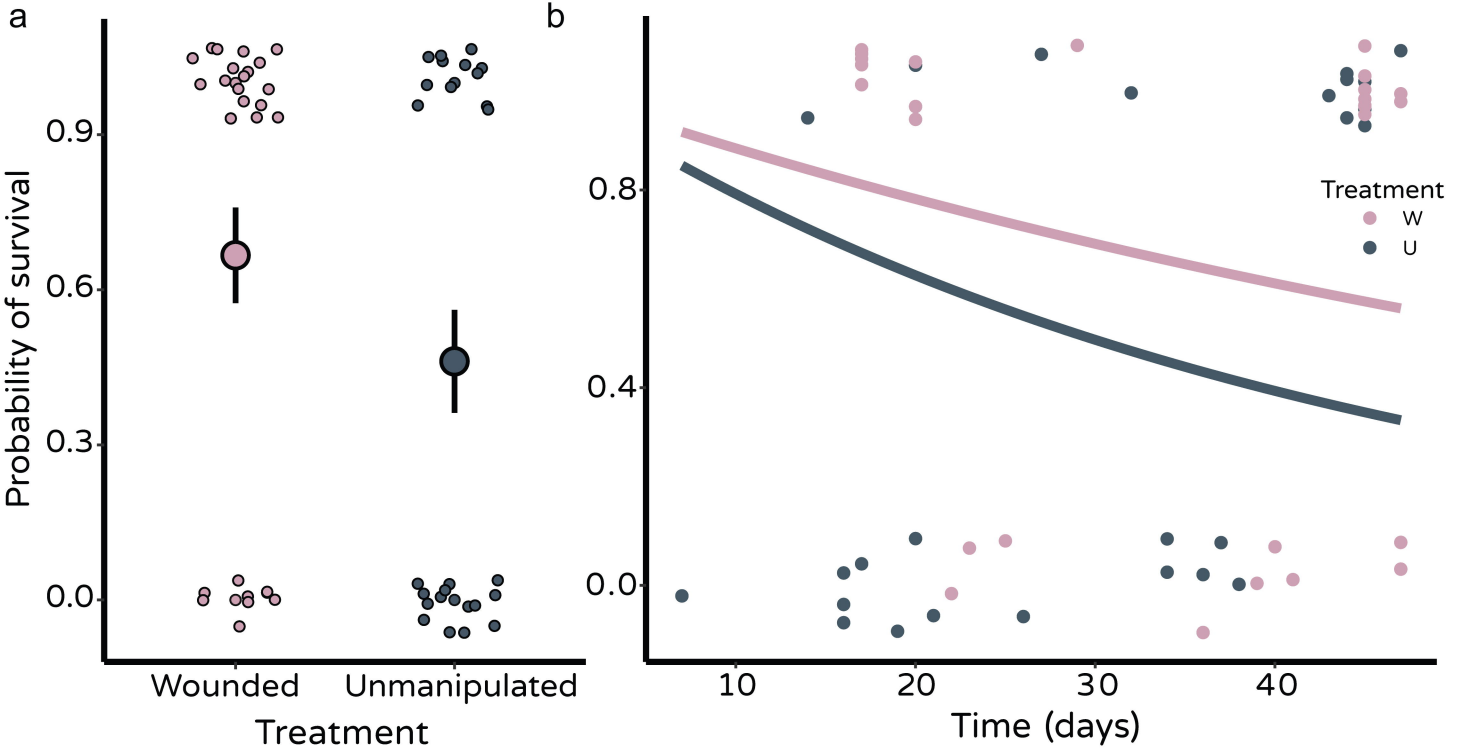
a
b
Probability of survival
0.0
0.3
0.6
0.9
Wounded
Unmanipulated
Treatment
0.0
0.4
0.8
10
20
30
40
Time (days)
Treatment
W
U

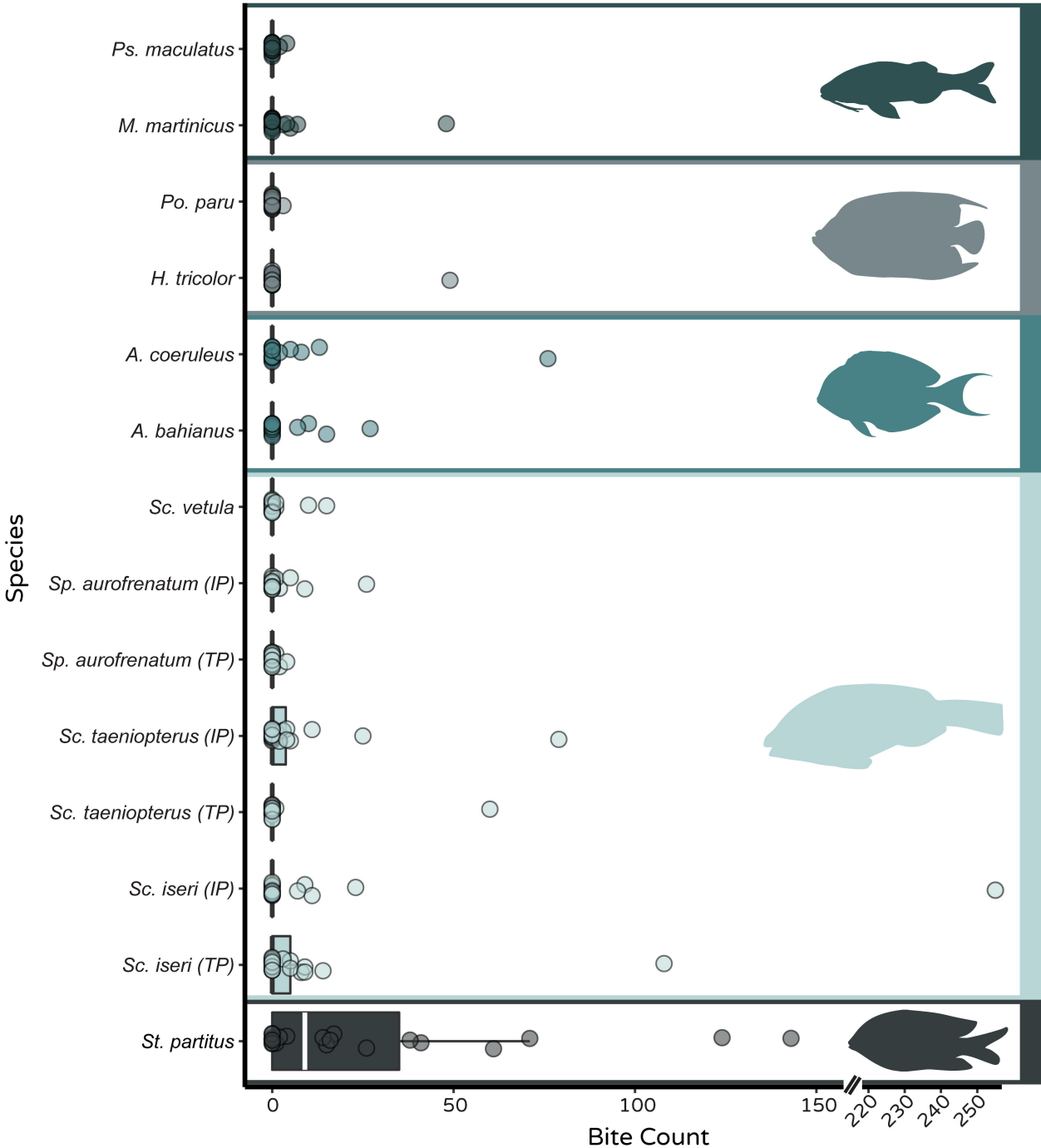
Ps. maculatus
M. martinicus
Po. paru
H. tricolor
A. coeruleus
A. bahianus
Sc. vetula
Sp. aurofrenatum (IP)
Sp. aurofrenatum (TP)
Sc. taeniopterus (IP)
Sc. taeniopterus (TP)
Sc. iseri (IP)
Sc. iseri (TP)
St. partitus
Species
0
50
100
150
220
230
240
250
Bite Count

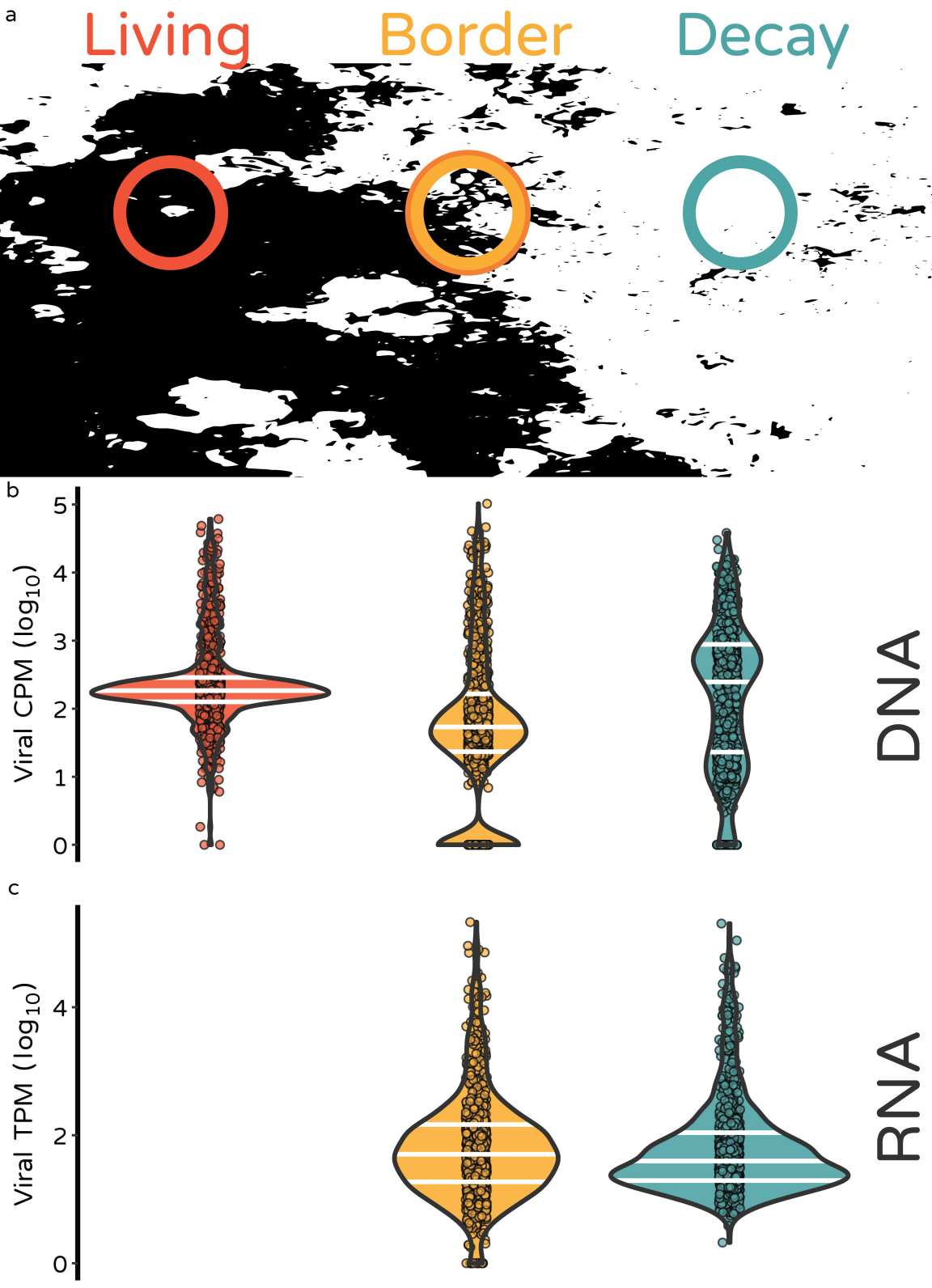
a
Living
Border
Decay
b
Viral CPM (log10)
5
4
3
2
1
0
DNA
c
Viral TPM (log10)
4
2
0
RNA

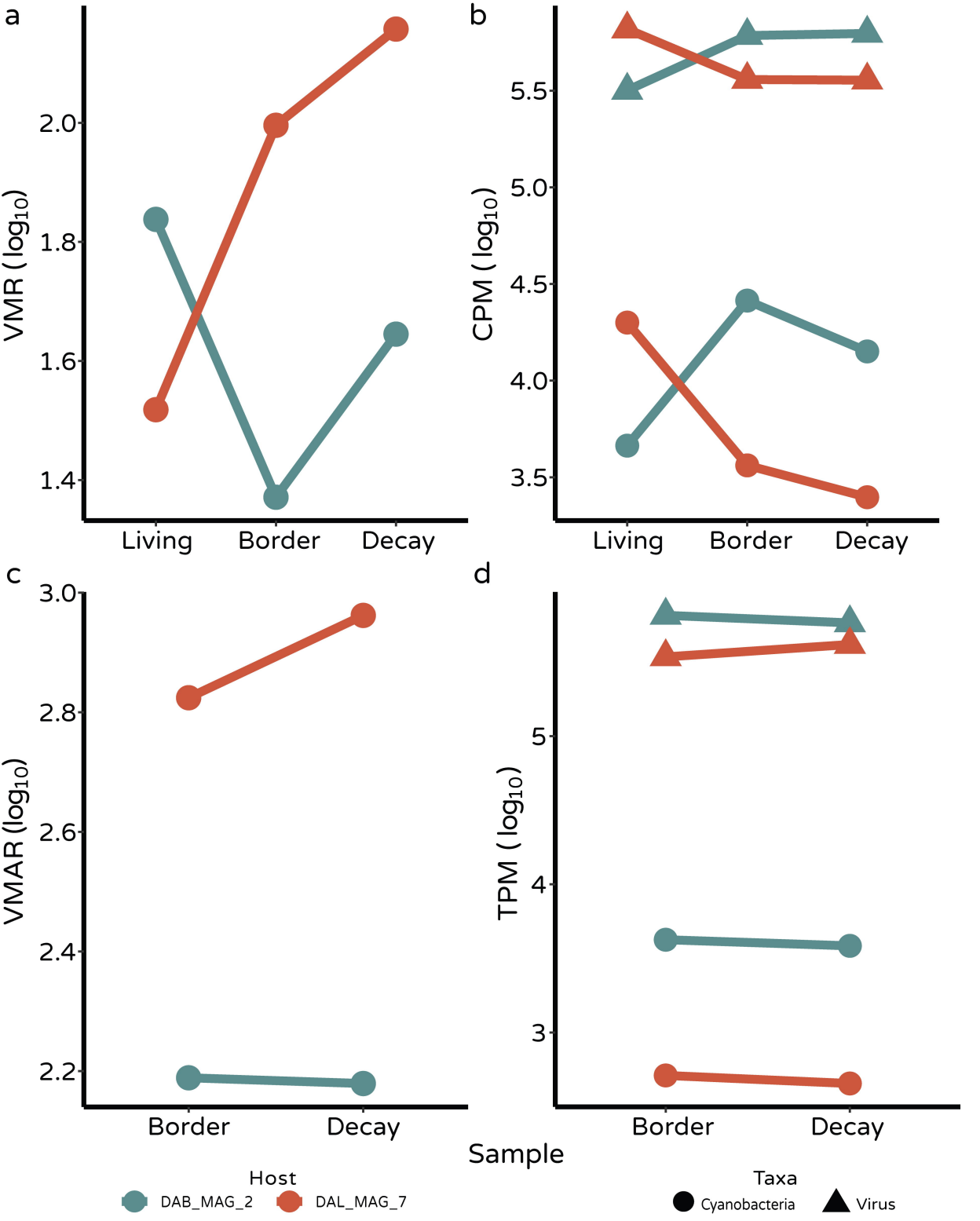
a
VMR (log10)
2.0
1.8
1.6
1.4
Living
Border
Decay
b
CPM (log10)
5.5
5.0
4.5
4.0
3.5
Living
Border
Decay
c
VMAR (log10)
3.0
2.8
2.6
2.4
2.2
Border
Decay
d
TPM (log10)
5
4
3
Border
Decay
Sample
Host
DAB_MAG_2
DAL_MAG_7
Taxa
Cyanobacteria
Virus

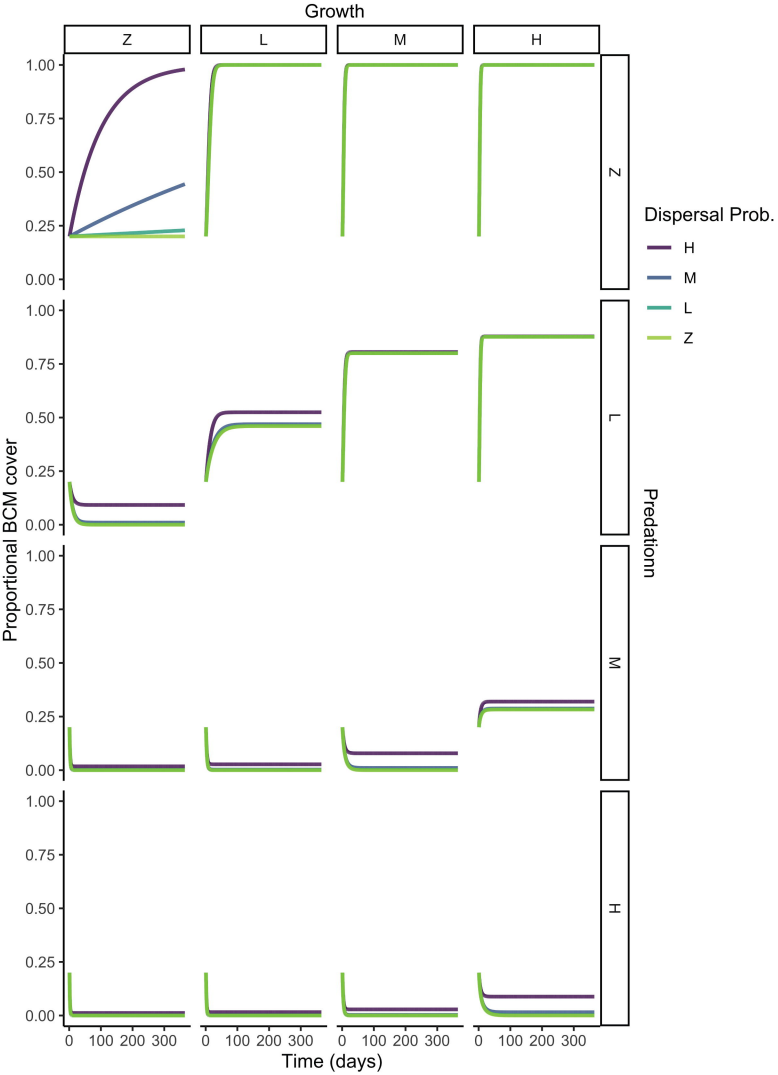
Growth
Z
L
M
H
Predationn
Z
L
M
H
Proportional BCM cover
1.00
0.75
0.50
0.25
0.00
0
100
200
300
Time (days)
Dispersal Prob.
H
M
L
Z